MINE ELECTRICAL POWER SYSTEMS

Transients Protection, Reliability Investigation, and Safety Testing of Mine Electrical Power Systems

VOL. III—OPTIMAL DESIGN OF MINE ELECTRICAL POWER SYSTEMS

Prepared for
United States Department of Interior
Bureau of Mines

by
College of Engineering
West Virginia University
Morgantown, West Virginia 26506

West Virginia University

Final Report for June 24, 1974 to August 15, 1978
on
Grant No. G0144137

August, 1979

50272-101

REPORT DOCUMENTATION PAGE	1. REPORT NO.	2.	3. Recipient's Accession No.
4. Title and Subtitle: Transients Protection, Reliability Investigation, and Safety Testing of Mine Electrical Power Systems, Vol. III-Optimal Design of Mine Electrical Power Systems			5. Report Date: Prepared Aug. 1979 6.
7. Author(s): M. M. Hassan and E. K. Stanek			8. Performing Organization Rept. No.
9. Performing Organization Name and Address: West Virginia University Department of Electrical Engineering Morgantown, WV 26506			10. Project/Task/Work Unit No. 11. Contract(C) or Grant(G) No. (C) (G) G0144137
12. Sponsoring Organization Name and Address: U.S. Department of the Interior, Bureau of Mines Interior Building Washington, D.C. 20240			13. Type of Report & Period Covered: Final Report 1974-1978 14.

15. Supplementary Notes

16. Abstract (Limit: 200 words)

This report describes the analysis tools developed at West Virginia University which can be implemented to optimally design coal mine electrical systems.

The basic analytical tools for all power systems are the load-flow and short-circuit analysis. Well known programs have been developed for analysis of ac transmission and distribution systems, but they are not applicable to a system which has combined ac/dc distribution, such as a coal mine power system. Furthermore, the topology of a coal mine electrical system changes continuously due to the movement of the locomotives on the track.

In the first section of this report, algorithms for carrying out load-flow and short-circuit analysis of a coal mine electrical system are described. Results from the study of a typical coal mine system are presented.

In the second section a method is described to optimally size power cables for cyclic loads. The method is based on the development of a thermal-electric model for a low-voltage power cable. Results from experimental verification of the model are also presented.

These techniques are useful in the safe, efficient, reliable and economical design of the coal mine electrical power systems.

17. Document Analysis a. Descriptors

Load flow analysis, short circuit analysis

b. Identifiers/Open-Ended Terms

c. COSATI Field/Group

18. Availability Statement	19. Security Class (This Report)	21. No. of Pages
Release unlimited	UNCLASSIFIED	55
	20. Security Class (This Page) UNCLASSIFIED	22. Price

(See ANSI-Z39.18) See Instructions on Reverse

OPTIONAL FORM 272 (4-77)
(Formerly NTIS-35)
Department of Commerce

Disclaimer Notice

The views and conclusions contained in this document are those of the authors and should not be interpreted as necessarily reflecting the official policies or recommendations of the Interior Department's Bureau of Mines or the U. S. Government.

TRANSIENTS PROTECTION, RELIABILITY INVESTIGATION, AND SAFETY TESTING OF MINE ELECTRICAL POWER SYSTEMS

VOL. III - OPTIMAL DESIGN OF MINE ELECTRICAL POWER SYSTEMS

Prepared for

UNITED STATES DEPARTMENT OF THE INTERIOR
BUREAU OF MINES

by

WEST VIRGINIA UNIVERSITY
MORGANTOWN, WV 26506

Final Report
Contract No. G0144137
Transients Protection, Reliability Investigation,
and Safety Testing of Mine Electrical Power Systems

August, 1979

FOREWORD

This report was prepared by West Virginia University, Department of Electrical Engineering, Morgantown, WV, under USBM Contract Number G0144137. The contract was initiated under the Health and Safety Program. It was administered under the technical direction of the Pittsburgh Mining and Safety Research Center with Mr. George J. Conroy acting as Technical Project Officer. Mr. H. Eveland was the contract administrator for the Bureau of Mines. This report is a summary of the work recently completed as a part of this contract during the period June 1974 to August 1978. This report was submitted by the authors in August, 1979.

VOL III - OPTIMAL DESIGN OF MINE ELECTRICAL POWER SYSTEMS

TABLE OF CONTENTS

CHAPTER I

INTRODUCTION

Some previous work has been done in the safety and reliability analysis of coal mine power systems. The major goal of this research is to use the existing information and generate additional information whenever necessary to optimally design coal mine power systems. The optimally designed power system would be reliable, economical and safe to operate. Since the topology of the coal mine power system is quite different from most of the utility-type systems, the analysis techniques available for these systems are not generally applicable to coal mine systems.

In the 1976-77 annual report a load-flow program for a combined ac/dc distribution system was described. However, this program is suitable for a system whose topology is fixed. But such is not the case with coal mine systems, where the dc system is constantly changing due to the movement of the locomotives or the track. This load flow program has been modified to take into account changing system conditions. Also, an ac/dc short circuit analysis program has been developed. To verify the results obtained by computer analysis, a small scale model of a coal mine power system has been built. Work has also proceeded to design a program to optimally size power cables for cyclic loads such as continuous miners, etc.

CHAPTER II

AC/DC LOAD-FLOW ANALYSIS

2.1 INTRODUCTION

In the 1976-77 annual report an ac/dc load flow program was described. The algorithm has been modified to take into account the actual rectifier characteristics and also the changing topology of the dc system. Also, modifications were carried out to achieve faster convergence.

2.2 MODEL OF THE THREE-PHASE RECTIFIER

The rectifier is an important element of the ac/dc system, since it converts ac power into dc. It can either be controlled (with ignition delay) or uncontrolled, as is the case in a mine power system. The analysis developed here pertains to the uncontrolled case, but can be used in the controlled case with minor modifications. The circuit diagram of a three-phase bridge rectifier is given in Fig. 2.1.

The approximate relationship[3] between the quantities on the ac and dc side are given by:

$$V_d = 1.35\ V_L \cos \alpha$$

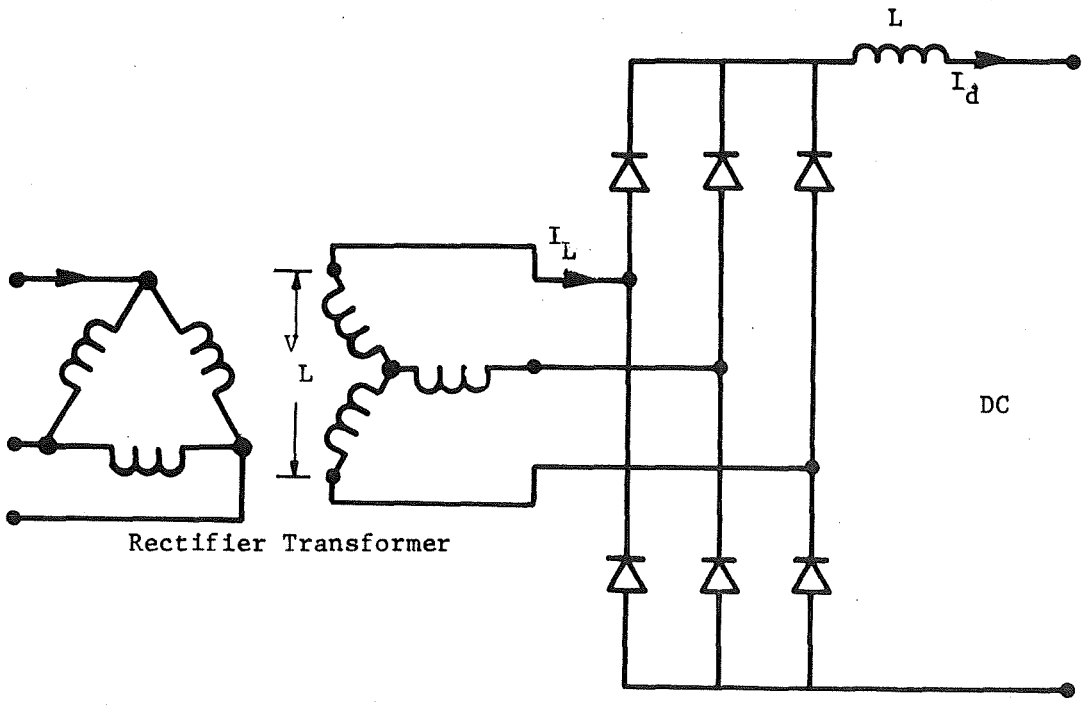

Fig. 2.1. Three-Phase Bridge Rectifier Circuit.

$$I_d = 1.282\ I_L$$

where

V_d is the no load dc voltage

I_d is the dc current

V_L is the rms values of line-to-line voltage on the secondary of the rectifier transformer.

I_L is the rms value of ac line current

α is the ignition delay angle (=0 in the uncontrolled case)

The approximate equivalent circuit of the rectifier is given in Fig. 2.2 This circuit representation is valid only in the per-unit system with an appropriate choice of the base values. It is also assumed that the losses in the rectifier are negligible.

It turns out that the per unit value of the voltage on dc side = CV where C is a conversion factor for the rectifier and V is the per unit value of the voltage on the ac side.

It can be shown that [3]

$$C \simeq \cos \phi$$

where ϕ is the phase angle between the voltage and current on the ac side of the rectifier and is dependent on the current through it. Thus the rectifier can be considered to have a fixed current ratio and an adjustable voltage ratio.

The voltage-current characteristics for an uncontrolled rectifier are given in Fig. 2.3.

The abscissa (I'_d) is the per unit value of dc current and the ordinate (V'_d) is the per unit value of the output dc voltage. However, it must be noted that the base current for the purpose of this curve is the short circuit current for a phase-to-phase fault on the secondary side of the rectifier transformer ($= \frac{\sqrt{3}\,E_m}{2\omega L_c}$) where E_m is the peak value of ac line-to-neutral voltage and L_c is the transformer leakage inductance. Thus, in order to convert the value of the current given by the curve to the system base, one has to use an appropriate conversion factor. The expression for these factors is derived below.

Let I_S be the base current on the short circuit base (A)

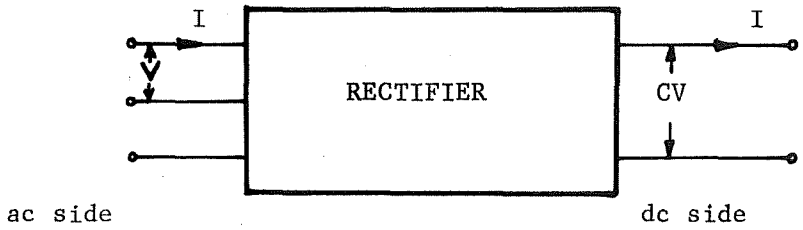

Fig.2.2 Equivalent Circuit for the Rectifier.

V is the per unit value of the voltage on the ac side.

I is the per unit value of the current on the ac side. It remains the same on the dc side.

CV is the per unit value of voltage on the dc side.

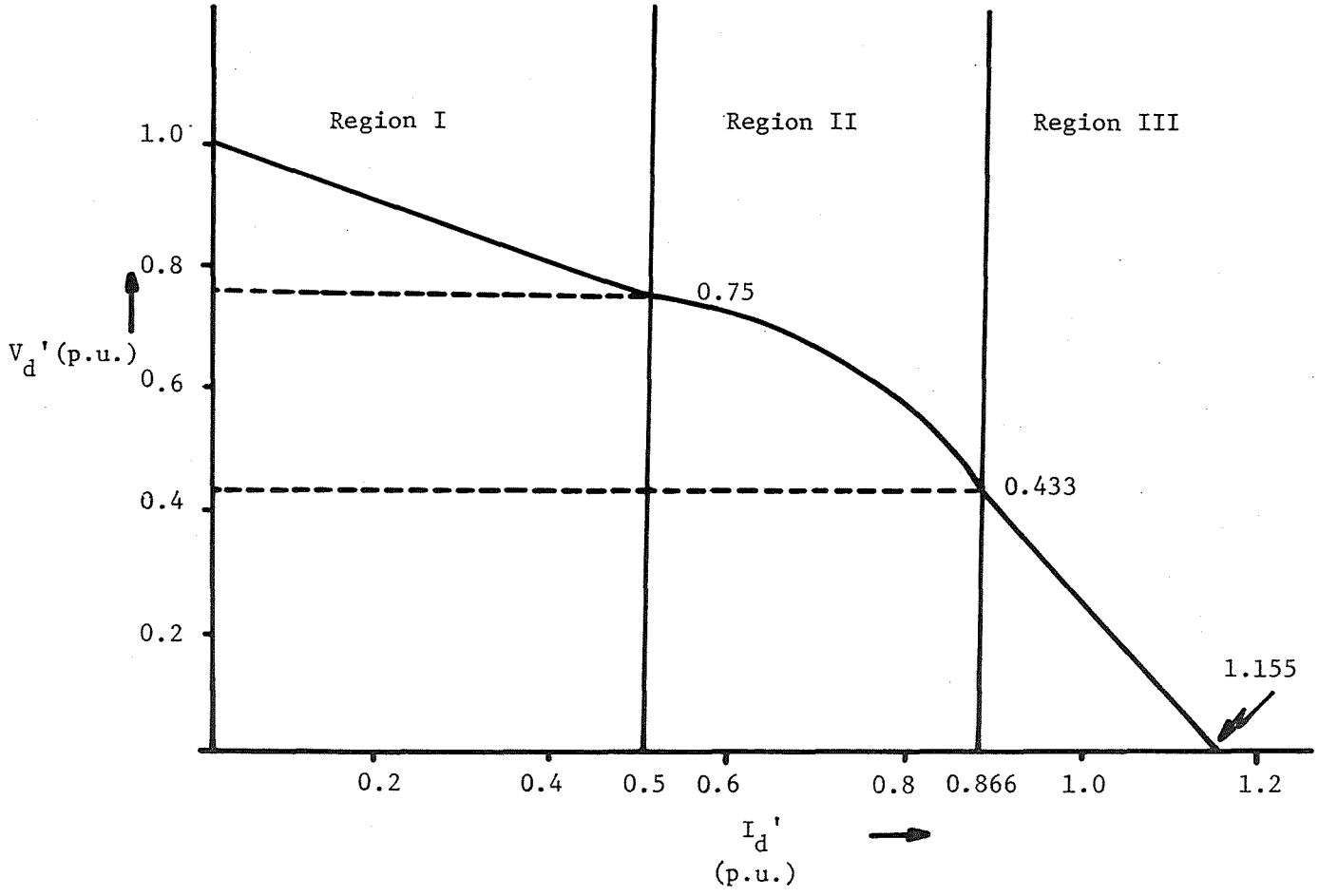

Fig. 2.3. Rectifier Voltage-Current Relationship for the Uncontrolled Case.

X the per unit reactance of the rectifier transformer on its own base
X_c be the reactance of rectifier transformer (Ω)
R be the rating of rectifier transformer (MVA)
P be the system base power (MVA)
V be the nominal value of the ac line-to-line voltage on the secondary side of rectifier transformer (kV)
V_A be the actual ac line-to-line voltage on the secondary of the rectifier transformer (kV)
E be the per unit value of the voltage on the secondary of the rectifier transformer
I_D be the per-unit dc current (on system base)

Now, the reactance of the rectifier transformer is

$$X_c = \frac{(V)^2 X}{R} \tag{2.1}$$

Also, the base current on short-circuit base

$$I_s = \frac{\sqrt{3}\ \sqrt{2}\ V_A}{2\sqrt{3}\ X_c} \times 10^3$$

$$= \frac{V_A\ R}{\sqrt{2}\ [V]^2 X} \times 10^3 \tag{2.2}$$

$$\text{System base current (dc)} = \frac{P \times 10^3}{1.35V}$$

$$\text{Thus, actual dc current} = \frac{P \times 10^3 \times I_D}{1.35V} \tag{2.3}$$

From equations 2.2 and 2.3 per-unit current on the short-circuit base

$$= \frac{\sqrt{2} P I_D\ V^2\ X}{1.35\ V\ V_A\ R}$$

$$= \frac{1.0475\ P\ I_D X}{RE} \tag{2.4}$$

As can be seen from the rectifier characteristics of Fig.2.3 there are three distinct regions of operation.

Region I

$\alpha = 0$

α increases from 0 to 60°

I'_d increases from 0 to 0.500

V'_d decreases linearly from 1 to 0.750

where α is the ignition delay angle

u is the angle of overlap

V'_d, I'_d are as defined earlier

Region II

α increases from 0 to 30°

u = 60°

I'_d increases from 0.500 to 0.866

V'_d decreases from 0.750 to 0.433 according to the relation

$$V'^2_d = (1-I'^2_d)\ 0.75$$

Region III

α = 30°

u increases from 60° to 120°

I'_d increases from 0.866 to 1.155

V'_d decreases linearly from 0.433 to 0

Thus, knowing the current flowing through the rectifier, one can find the conversion factor for the voltage. It may be noted here that during normal operation the rectifier operates in the linear region (Region I). Only during an abnormal condition, such as a short circuit, will the rectifier operate in Regions II or III.

2.3 FORMATION OF ALGORITHUM FOR LOAD-FLOW ANALYSIS

Using the rectifier characteristics discussed above one can write the system equations for performing the load flow analysis on a combined ac/dc system. The analysis starts by dividing the whole network into three kinds of buses.

1. Pure ac buses, which are a part of the ac system but not connected to any of the rectifiers.
2. Transfer buses, which are connected to the rectifier.
3. Pure dc buses, which are a part of the dc system but not connected to any of the rectifiers.

The network equations are written and solved iteratively using the Gauss-Seidel procedure. This method is chosen because of its simplicity and also due to the fact that the product of the computation time per iteration and number of iterations is very small.

The real and reactive power at any bus p is

$$P_p - jQ_p = E_p^* I_p$$

and the current is

$$I_p = \frac{P_p - j Q_p}{E_p^*} \tag{2.5}$$

where I_p is positive, flowing into the system.

Let N_{AC} be the number of pure ac buses.

N_T be the number of transfer buses (number of rectifiers).

N_{DC} be the number of pure dc buses.

then

Effective number of ac buses, $N_A = N_{AC} + N_T$

Effective number of dc buses, $N_D = N_{DC} + N_T$

The system is hypothetically broken up at each of the transfer buses with some unknown real power being injected into the dc system. The concept of breaking the network into two subnetworks can be explained with reference to Fig. 2.4, Fig. 2.4a shows the composite network. The ac network injects real power into the dc network at the transfer buses. Then, viewed from the ac side the dc network can be represented as an unknown load at the transfer buses (Fig. 2.4b). Similarly, viewed from the dc side, the ac network can be represented as injecting real power into the dc network (Fig. 2.4c). Thus, the two networks are effectively isolated. The performance of the network can be obtained from the equations:

$$[I_{BUS(ac)}] = [Y] [E_{BUS(ac)}] \tag{2.6}$$

$$[I_{BUS(dc)}] = [y] [E_{BUS(dc)}] \tag{2.7}$$

where [Y] and [y] are the bus admittance matrices for the ac and dc networks, respectively.

The solution of the load flow problem is initiated by assuming voltages for all the buses, except the slack bus where the voltage is specified and remains fixed. The slack bus in a typical mine power system would be the point of connection to the utility.

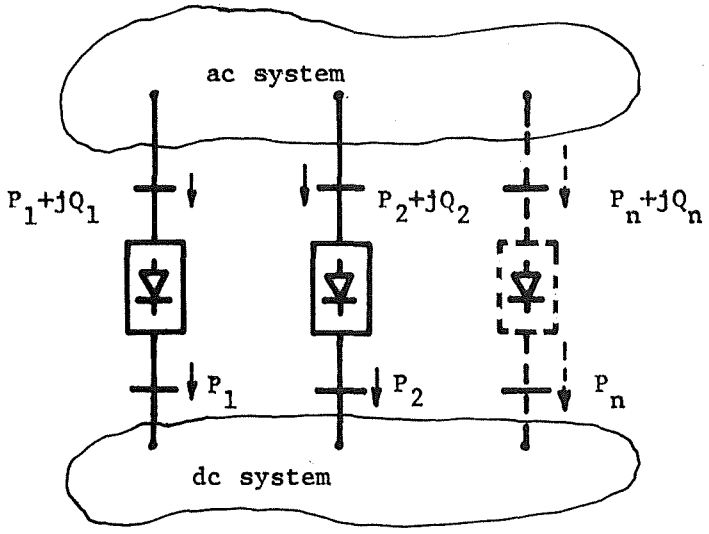

Fig. 2.4a. Composite ac/dc System.

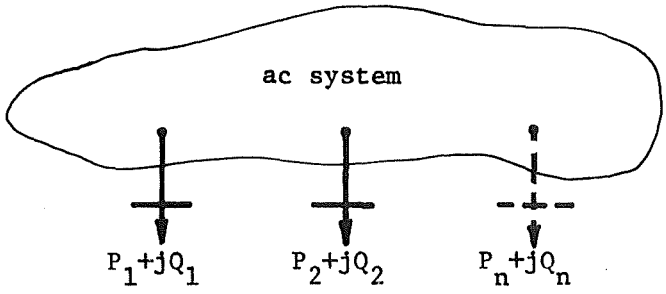

Fig. 2.4b. The Pure ac System, with the dc System Acting as a Load at the Transfer Buses.

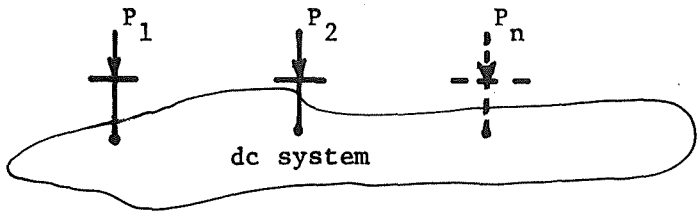

Fig. 2.4c. The Pure dc System with Real Power Being Injected at the Transfer Buses.

It may be noted here that the transfer buses are numbered sequentially before the pure dc buses when considering the dc network. The same sequence is followed in numbering the transfer buses in the ac network, except that they are numbered after the pure ac buses. The slack bus is numbered 1.

Selecting ground as the reference one can write for the pure ac buses $(p=2,\ldots N_{AC})$

$$E_p = \frac{1}{Y_{pp}} \left[I_p - \sum_{\substack{q=1 \\ q\neq p}}^{N_A} Y_{pq} E_q \right] \tag{2.8}$$

The network equations 2.8 and the bus loading equations 2.5 can be combined to obtain:

$$E_p = \frac{1}{Y_{pp}} \left[\frac{P_p - j Q_p}{E_p^*} - \sum_{\substack{q=1 \\ q\neq p}}^{N_A} Y_{pq} E_q \right] \tag{2.9}$$

Thus, knowing the initial values of the voltages, one has a new estimate for the voltages of pure ac buses.

Similarly, for the pure dc buses $(p=N_T+1,\ldots N_D)$

$$E_p = \frac{1}{Y_{pp}} \left[\frac{P_p}{E_p} - \sum_{\substack{q=1 \\ q\neq p}}^{N_D} y_{pq} E_q \right] \tag{2.10}$$

For the transfer buses $(p=N_{AC}+1,\ldots N_A)$

$$E_p = \frac{1}{Y_{pp}} \left[\frac{P_p - j Q_p}{E_p^*} - \sum_{\substack{q=1 \\ q\neq p}}^{N_A} Y_{pq} E_q \right] \tag{2.11}$$

where $(P_p - j Q_p)$ is the power flow into the rectifier.

Now

$$P_p - j Q_p = P_p - j P_p \operatorname{Tan} (\cos^{-1} C_p) \tag{2.12}$$

where C_p is the voltage conversion factor for the rectifier connected to bus p.

Since the transfer buses are a part of the dc network too, one can write

$$C_p |E_p| = \frac{1}{y_{pp}} \left[\frac{-P_p}{|E_p|} - \sum_{\substack{q=1 \\ q\neq p}}^{N_D} y_{pq} E_q \right] \quad p=1,\ldots N_T \tag{2.13}$$

Thus,

$$P_p = - C_p\, y_{pp}\, |E_p|^2 - |E_p| \sum_{\substack{q=1 \\ q\neq p}}^{N_D} y_{pq}\, E_q \qquad p = 1,\ldots N_T \tag{2.14}$$

which gives the real power injected into the dc system at each transfer bus.

Substituting equation 2.14 in 2.12 one obtains for the transfer buses $(p=N_{AC}+1,\ldots..N_A)$

$$E_p = \frac{1}{Y_{pp}} \left[\frac{1}{E_p^*} \left[- C_p\, y_{pp}\, |E_p|^2 - |E_p| \sum_{\substack{q=1 \\ q\neq p}}^{N_D} y_{pq}\, E_q \right] \left[1 - j \tan(\cos^{-1} C_p)\right] - \sum_{\substack{q=1 \\ q\neq p}}^{N_A} Y_{pq}\, E_q \right] \tag{2.15}$$

Note that this equation for the transfer buses is independent of the bus power. Knowing the initial estimates for the bus voltages and conversion factors for the rectifiers, the new estimates for the transfer bus voltages can be obtained.

However, before the next iteration can be performed, one has to have a new estimate for conversion factors for each of the rectifiers in the system. This can be done as follows.

Using equation 2.14 find P_p for each transfer bus. This will give the real power injected into the dc system at each transfer bus. Then, the total power injected into the dc system is given by:

$$P_{TOTAL} = \sum_{p=1}^{N_T} P_p \tag{2.16}$$

When the solution finally converges

$$P_{TOTAL} = P_{LOSS} + P_{LOAD} \tag{2.17}$$

where

P_{LOSS} = power loss in the dc system

P_{LOAD} = total load on the dc system

and

$$P_{LOSS} = \Sigma(E_p - E_q)^2 \, ys_{pq} \tag{2.18}$$

where ys_{pq} is the self admittance of the element connected between bus p and bus q. The summation is carried out over the entire dc network.

At each iteration the bus power mismatch ΔP is given by:

$$\Delta P = P_{TOTAL} - (P_{LOSS} + P_{LOAD}) \tag{2.19}$$

This power mismatch has to be alloted to the various transfer buses. The new bus powers can be calculated as:

$$P_p = P_p + \left(\frac{\Delta P}{P_{TOTAL}}\right) P_p \qquad p=1,\ldots N_T \tag{2.20}$$

Knowing the new bus powers, the currents through the various rectifiers can be calculated as:

$$I_p = \frac{P_p}{|E_p|} \qquad p=1,\ldots N_T \tag{2.21}$$

Once the currents are known, the new estimates for the rectifier conversion factors are found from rectifier characteristics (Fig.2.3). This completes one iteration of the solution. This process is repeated, until the bus voltages have converged to the required tolerance. Once the final voltages have been determined, the line flows can easily be calculated.

2.4 MODIFICATIONS FOR MOVING LOADS

In the preceding analysis it was assumed that the dc network topology remains fixed. But such is hardly the case. In a real system, the dc loads, such as locomotives on the track are in a state of constant motion. Hence, the network topology is constantly changing. It is very difficult to solve the system on a continuous basis. As such, a time step approach is preferred. At each time step the system is assumed to be fixed in a particular state depending upon the positions of the locomotives. To solve for the system at each time step the following procedure is followed:

1. Knowing the position of the vehicle and the vehicular dynamics, the power requirements are calculated. For ease of calculation the track is assumed to be piece-wise linear (slope-wise).
2. The elements of the bus admittance matrix for the dc network are suitably modified.
3. Load flow analysis (as already outlined) is performed and a solution obtained at each time step.

2.5 VEHICLE POWER REQUIREMENTS

The tractive effort needed to pull a locomotive is given by:

$$F = F_d + (F_a + F_r + F_g)\, W_g \tag{2.22}$$

where

F is the tractive effort, in lbs

F_d is the air drag, in lbs, ($= \frac{C_d\, \zeta\, V^2 A}{2}$)

C_d is drag coefficient

ζ = .002378 lb sec^2/ft^4

V is vehicle speed, in ft/sec

A is vehicle frontal area, in ft^2

F_a is the force to accelerate, in lbs/ton, (= 2000(a/g)

a is the maximum acceleration

g = 32.2 ft/sec^2

F_r is force to overcome track resistance, in lbs/ton

F_g is the force to overcome grade resistance, in lbs/ton = 20 G

G is the percentage grade

W_g is the gross vehicular weight, in tons

The horse power requirements are given by

$$H.P. = \frac{FxV}{550\eta} \tag{2.23}$$

where η is the efficiency of the system.

2.6 MODIFICATIONS IN BUS ADMITTANCE MATRIX FOR A MOVING LOAD

As the locomotive travels along the track, the bus admittance matrix for the dc network is constantly changing. However, for the load flow solution, the elements of the bus admittance matrix have to be modified at each time step only, since a time step approach is used.

Referring to Fig. 2.5 consider a locomotive between buses i and j at a distance x(t) ft from bus i at any instant of time t. Let the locomotive bus be named k. Also, let X be the length of track between i and j in ft and R be the per unit resistance of the track (trolley wire and return) per foot of its length.

The modified elements of the bus admittance matrix are calculated as follows. The old values refer to the parent network.

$$y(i,i) = y(i,i)\ \text{old} + \left(\frac{1}{x(t)} - \frac{1}{X} \right) /R \tag{2.24}$$

$$y(j,j) = y(j,j)\ \text{old} + \left(\frac{1}{X-x(t)} - \frac{1}{X} \right) /R \tag{2.25}$$

$$y(i,j) = y(j,i) = 0 \tag{2.26}$$

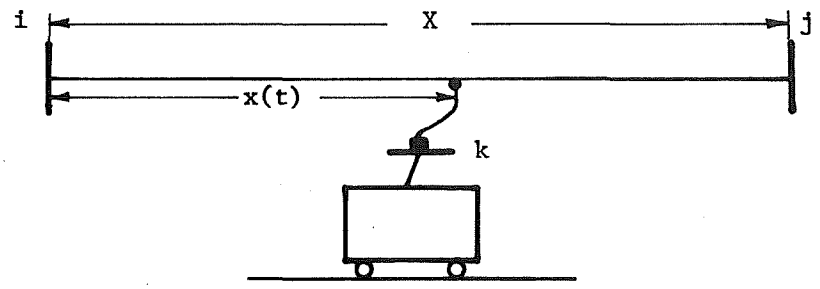

Fig. 2.5 Locomotive on Track.

$$y(k,k) = \frac{1}{XR} \tag{2.27}$$

$$y(k,i) = y(i,k) = -\frac{1}{x(t)R} \tag{2.28}$$

$$y(k,j) = y(j,k) = -\frac{1}{(X-x(t))\ R} \tag{2.29}$$

2.7 RESULTS FROM A SAMPLE SYSTEM

A computer program was written and tested for a sample system which is typical of a small coal mine. This system is shown in Fig.2.6 It has a total of 10 pure ac and 10 pure dc buses. There are five rectifiers feeding the dc system. Besides a number of ac loads, two locomotives are supposed to move along the track according to some pre-determined conditions. These conditions were not based on actual production schedules for a typical mine, because such a production model was not available.

Locomotive 1 was supposed to start at the location of rectifier B and move toward rectifier A and finally rectifier C. Locomotive 2 was supposed to start at the location of power-center 2 and move toward rectifier E and finally rectifier D. The time step for the solution was chosen as 5 seconds.

The program worked well, except that it took many iterations for convergence. The number of iterations for the first time step was approximately 150 (for a voltage tolerance of 10^{-4} per-unit) but decreased for subsequent time steps. This could be attributed to the radial nature of the power system. To accelerate the convergence of the iterative process, suitable acceleration factors were used. It was found that the convergence of solution was very sensitive to the magnitude of the acceleration factors. For the system under study a factor of 1.6 was found to be optimal. This may or may not be true for larger systems, which is a subject of further research.

Some of the results obtained from the analysis are given in Figs. 2.7 through 2.9. Fig. 2.7 gives the real and reactive power loading of the substation transformer as a function of time. Fig. 2.8 gives the loading of rectifier B. Fig. 2.9 gives the voltage across locomotive 1 as a function of time.

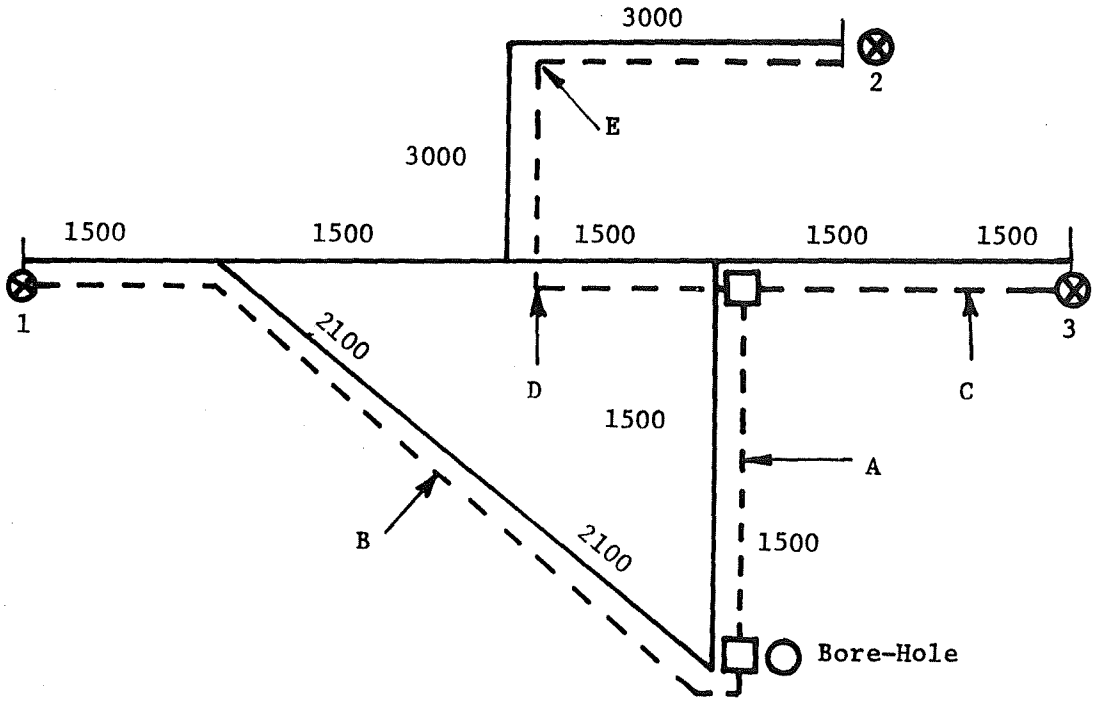

Rail haulage track

High-voltage distribution

Power center

Rectifier location

Switch-house

Notes:

1. All lengths are in feet.
2. Each power center has 200 kW of ac load through 4/0 cable at 0.6 power factor lag.
3. High voltage distribution is at 7200 V.
4. All high voltage cables are 1/0.

Fig. 2.6 Typical Mine System for Load Flow Study.

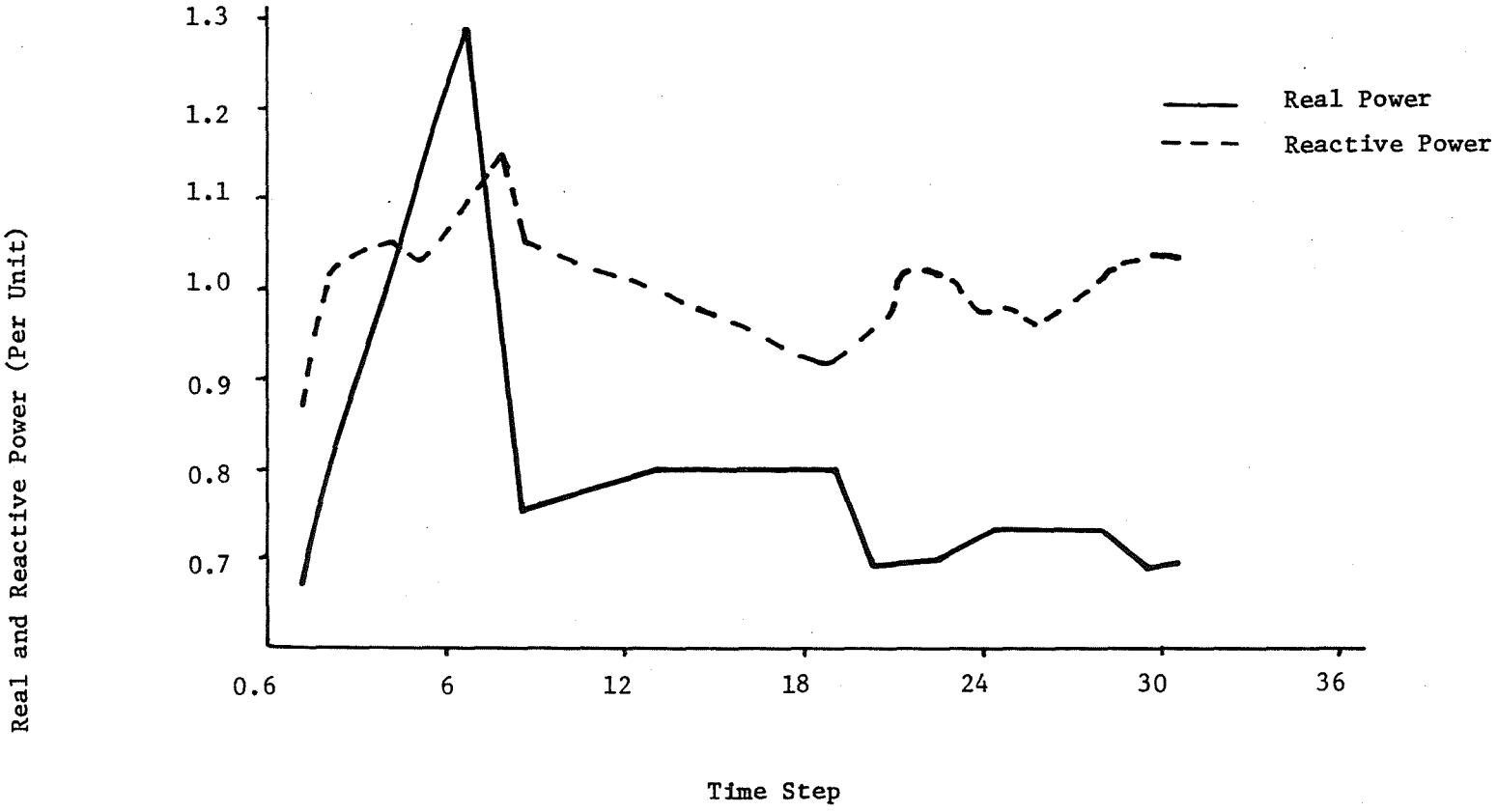

Fig. 2.7 Real and Reactive Power Loading of the Sub-Station Transformer as a Function of Time.

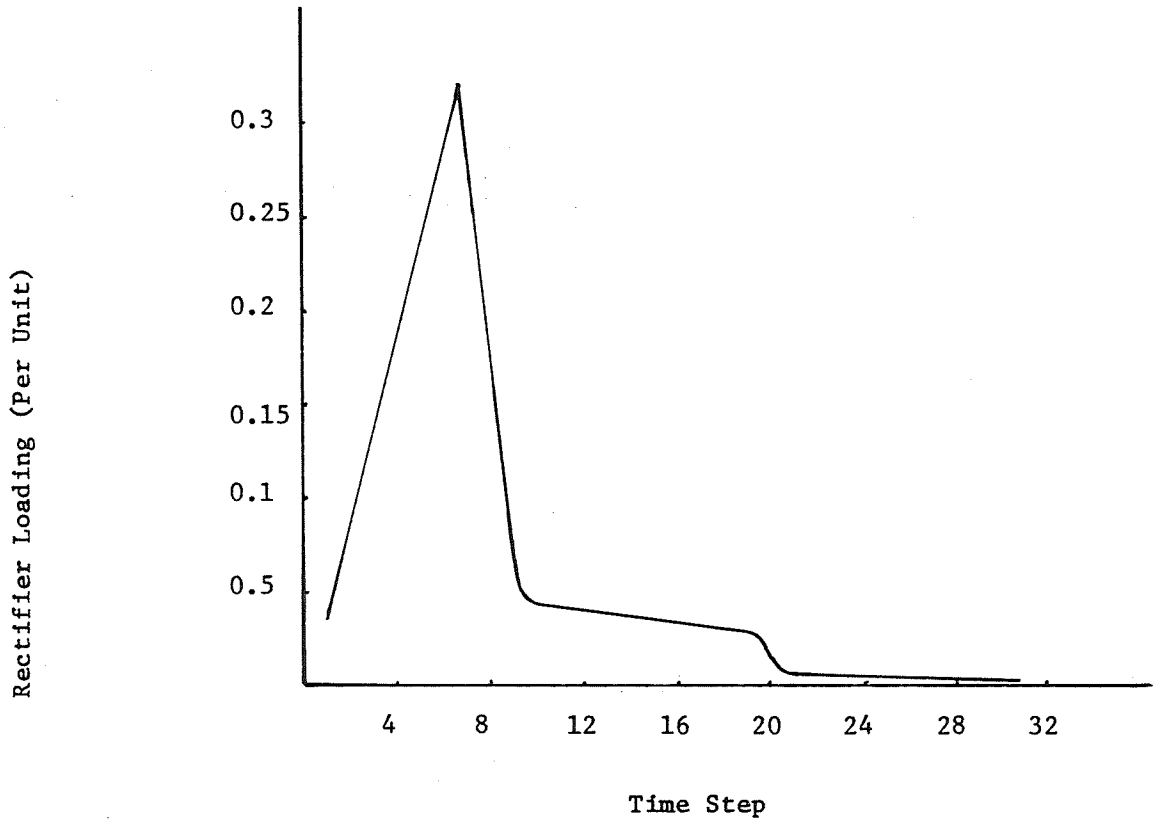

Fig. 2.8 Loading of Rectifier B as a Function of Time.

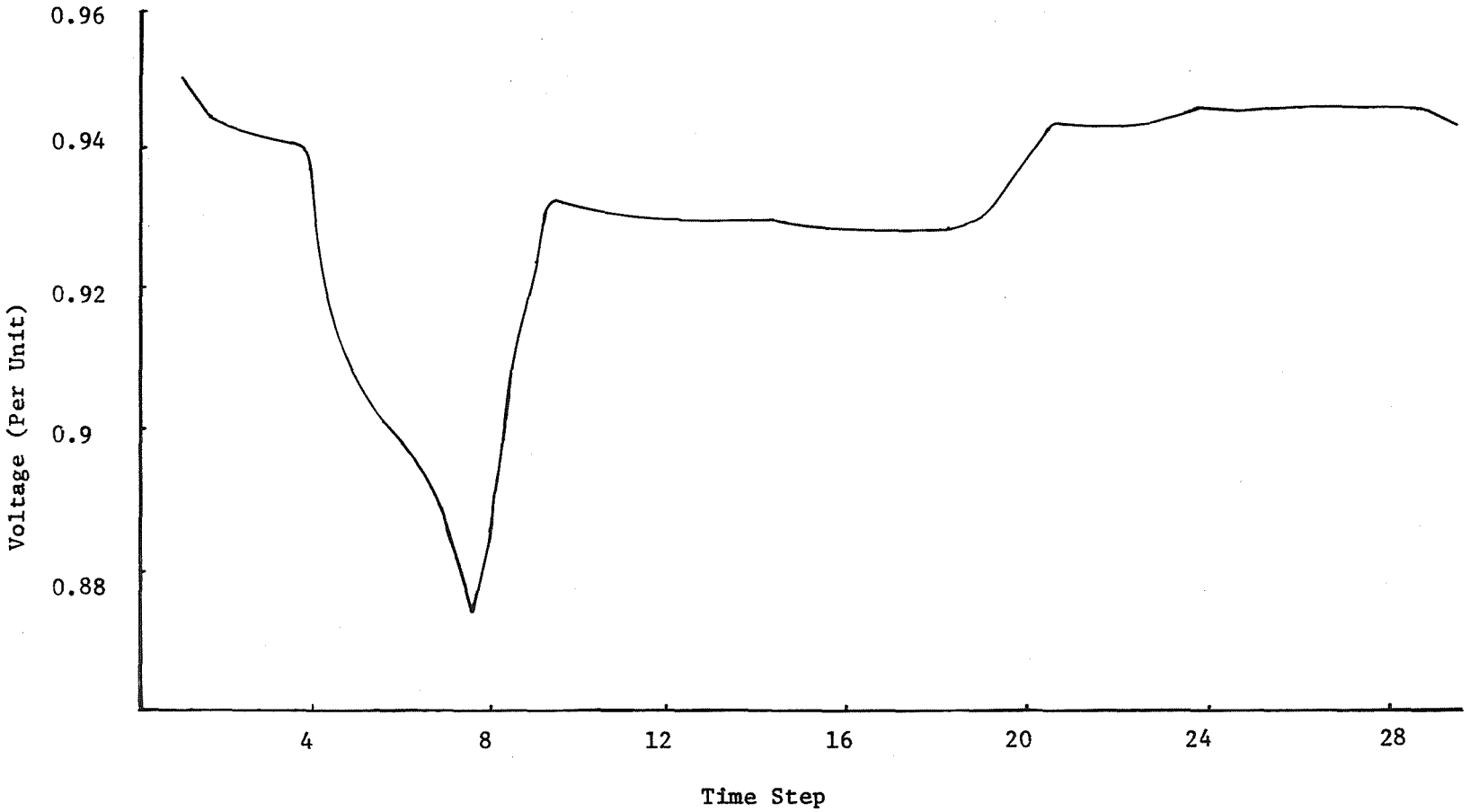

Fig. 2.9 Voltage Across Vehicle 1 as a Function of Time.

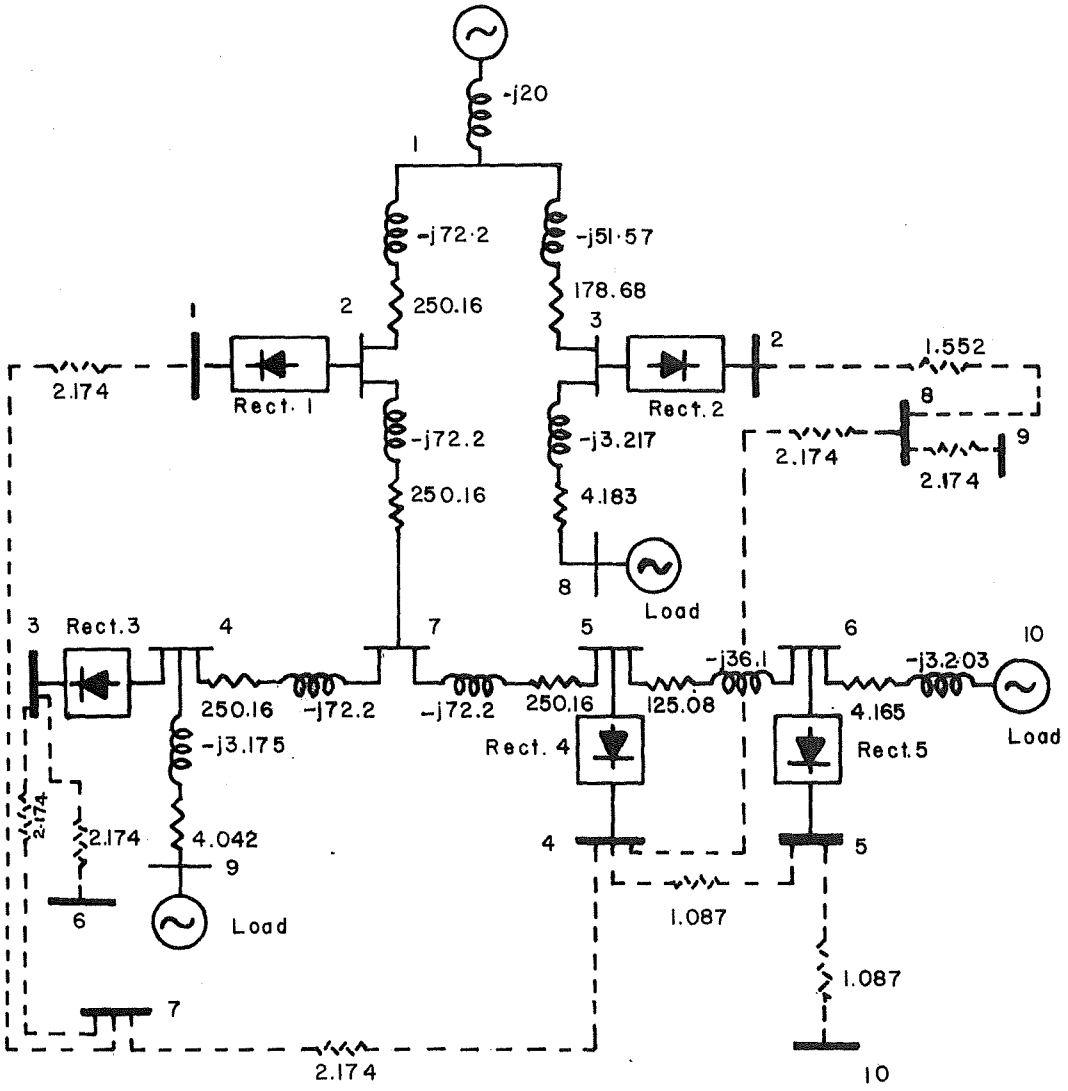

Fig. 2.10. Single Line Diagram of the Sample System (All Are Admittance Values in Per Unit of the System Base).

CHAPTER III

AC/DC SHORT CIRCUIT ANALYSIS

3.1 INTRODUCTION

This analysis provides information regarding currents and voltages on the power system during fault conditions. This information is helpful in designing a protective relaying scheme for the network and also in choosing the interrupting rating for the switching devices at each switching location. In this study, only faults on the dc network are considered. Faults on the ac network are covered by many textbooks on computer analysis of power systems.[4]

3.2 FAULT AT A REMOTE DC BUS

This analysis is valid for faults at any dc bus except the buses connected to the rectifiers. Before proceeding with the system equations, the following assumptions are made:

1. The pre-fault voltage at all the buses is the same and is constant.
2. All shunt connections, such as loads and line charging, are neglected.
3. All transformers are set at nominal taps.

For a short-circuit on the dc side, the fault current will flow through each of the rectifiers. As in the case of load flow, one can hypothetically break up the system at each of the rectifier buses, assuming that the fault current will be injected into the dc system at each rectifier bus.

If one forms the bus impedance matrix (Z_{BUS}) for the ac system, one can use Thevenin's theorem to represent the ac system during the fault. When forming Z_{BUS}, note that the buses have to be numbered in the following order.

1. The point of utility connection.
2. All the transfer buses.
3. Remaining ac buses.

The performance equations of the ac system during a fault is

$$E_{BUS(F)} = E_{BUS(O)} - Z_{BUS}\, I_{BUS(F)} \qquad (3.1)$$

where

$E_{BUS(F)}$ is the vector of bus voltages during the fault
$E_{BUS(O)}$ is the vector of pre-fault bus voltages
$I_{BUS(F)}$ is the vector of bus currents during the fault

Assuming the pre-fault bus voltages as 1+0j, equation 3.1 can be written in matrix form as:

$$\begin{bmatrix} E_1 \\ E_2 \\ \vdots \\ E_{N_T+1} \\ E_{N_T+2} \\ \vdots \\ E_{N_A} \end{bmatrix} = \begin{bmatrix} 1+j0 \\ \vdots \\ \vdots \\ \vdots \\ 1+j0 \end{bmatrix} - \begin{bmatrix} Z_{1,1} & \cdots & Z_{1,N_A} \\ Z_{2,1} & \cdots & Z_{2,N_A} \\ \vdots & & \vdots \\ Z_{N_T+1,1} & \cdots & Z_{N_T+1,N_A} \\ Z_{N_T+2,1} & \cdots & Z_{N_T+2,N_A} \\ \vdots & & \vdots \\ Z_{N_A,1} & \cdots & Z_{N_A,N_A} \end{bmatrix} \begin{bmatrix} 0 \\ I_2 \\ \vdots \\ I_{N_T+1} \\ 0 \\ \vdots \\ 0 \end{bmatrix} \tag{3.2}$$

where

E's are the bus voltages in vector form.
I's are the bus currents in vector form.
Z's are the elements of the bus impedance matrix for the ac network

In general

$$E_k = |E_k| \angle \delta_k \qquad k=1,\ldots N_A$$
$$I_i = |I_i| \angle (\delta_i - \phi_i) \qquad i=2,\ldots N_T+1$$

where

$|E_k|$ is the magnitude of ac voltage at bus k during the fault.
δ_k is the phase angle of the bus voltage.
$|I_i|$ the magnitude of the fault current at bus i.
ϕ_i is the phase angle between the voltage and current at bus i.
N_T, N_A are as defined earlier.

Equation 3.2 can be written in the following general form

$$|E_k| \angle \delta_k = 1 - \left[\sum_{i=2}^{N_T+1} Z_{k,i} \; |I_i| \; \angle (\delta_i - \phi_i) \right] \tag{3.3}$$

$k=1,2,\ldots N_A$

For a fault on the dc side, the current will be zero at every bus, except the transfer buses and the faulted bus. Starting with a bus admittance matrix for the original dc network, one can eliminate all the buses where the

current is zero, using the well-known technique of node elimination. When writing the bus admittance matrix one has to be careful to number the transfer buses first in the same sequence as followed on the ac side. The pure dc buses are numbered following the transfer buses.

One can write for the dc system:

$$\begin{bmatrix} |I_2| \\ |I_3| \\ \vdots \\ |I_{N_T+1}| \\ |I_F| \end{bmatrix} = \begin{bmatrix} Y'_{1,1} & \cdots & Y'_{1,N_T+1} \\ Y'_{2,1} & \cdots & Y'_{2,N_T+1} \\ \vdots & & \vdots \\ Y'_{N_T,1} & \cdots & Y'_{N_T,N_T+1} \\ Y'_{N_T+1,1} & \cdots & Y'_{N_T+1,N_T+1} \end{bmatrix} \begin{bmatrix} C_2 & |E_2| \\ C_3 & |E_3| \\ & \vdots \\ C_{N_T+1} & |E_{NT+1}| \\ & 0 \end{bmatrix} \tag{3.4}$$

In general

$$|I_i| = \left[\sum_{j=1}^{N_T} Y'_{i-1,j} \; C_{j+1} \; |E_{j+1}| \right] \tag{3.5}$$

$i=2,3\ldots N_T+1$

where

C_i is the voltage conversion factor for the rectifier connected to bus i ($C_i=\cos \phi_i$).

I_F is the magnitude of the current at the faulted bus.

Y''s are the elements of the bus admittance matrix for the reduced system.

One can combine equations 3.3 and 3.5 to obtain

$$|E_k| \angle\delta_k = 1 - \left[\sum_{i=2}^{N_T+1} Z_{k,i} \left(\sum_{j=1}^{N_T} Y'_{i-1,j} \; C_{j+1} \; |E_{j+1}| \right) \angle(\delta_i - \phi_i) \right] \tag{3.6}$$

$k=1,2,\ldots N_A$

This is a non-linear equation in terms of the bus voltages and rectifier conversion factors. One has to solve this equation iteratively in conjunction with the rectifier characteristics of Fig. 2.3 to obtain the final values of the ac bus voltages during the fault.

At this stage, the only voltages known for the dc network are those for the transfer buses. The rest of the voltages can be determined as follows:

One can write for the dc network

$$[I] = [y]\,[E] \tag{3.7}$$

where

I is a vector of bus currents.
E is a vector of bus voltages.
y is the bus admittance matrix for the original dc network.

in partioned form one can write (3.7) as:

$$\begin{bmatrix} I_1 \\ \hline I_2 \end{bmatrix} = \begin{bmatrix} y_{11} & y_{12} \\ \hline y_{21} & y_{22} \end{bmatrix} \begin{bmatrix} E_1 \\ \hline E_2 \end{bmatrix} \tag{3.8}$$

where

I_1 is a vector of bus currents at transfer buses and is known.

I_2 is a vector of bus currents at remaining dc buses (=0)

E_1 is a known vector of transfer bus voltages.

E_2 is a vector of dc bus voltages to be determined.

From equation (3.8) one can write:

$$[y_{21}]\,[E_1] + [y_{22}]\,[E_2] = 0$$

Thus

$$[E_2] = -\,[y_{22}]^{-1}\,[y_{21}]\,[E_1] \tag{3.9}$$

Thus all the voltages are determined. Once the voltages are known, the line flows can be easily calculated.

3.3 FAULT AT THE TERMINALS OF A RECTIFIER

The analysis becomes a little different when a fault occurs on the dc terminals of a rectifier.

Let the faulted rectifier be connected to bus N_F of the ac system. One can write an equation similar to (3.3) for the ac system

$$E_k \angle\delta_k = 1 - \left[\sum_{\substack{i=2 \\ i\neq N_F}}^{N_T+1} Z_{k,i}\,|I_i|\,\angle(\delta_i-\phi_i)\right] - Z_{k,N_F}\,|I_{N_F}|\,\angle(\delta_{N_F}-90^\circ) \tag{3.10}$$

$k=1,2,\ldots N_A$

where $|I_{N_F}|$ is the current through the faulted rectifier and can be calculated as shown below.

Let I_{SC} be the short circuit dc current (A) through the rectifier.

$$I_{SC} = \frac{\sqrt{2}\ V_A}{\sqrt{3}\ X_c} \times 10^3$$

$$= \frac{0.8165\ V_A\ R}{V^2\ X} \times 10^3 \qquad (3.11)$$

where

V_A is the actual voltage on the secondary of the rectifier transformer, in kV
X_c is reactance of rectifier transformer, in Ω
X is reactance of rectifier transformer, in per unit on its own base
R is rating of rectifier transformer, in MVA
V is the nominal secondary voltage of the rectifier transformer, in kV

$$\text{System base current (dc)} = \frac{P \times 10^3}{1.35\ V} \qquad (3.12)$$

where P is the system base power in MVA

Thus, rectifier short circuit current on system base

$$= \left(\frac{0.8165\ V_A\ R}{V^2\ X}\right) \left(\frac{1.35V}{P}\right)$$

$$= \frac{1.1022\ RE}{PX} \qquad (3.13)$$

where E is the per-unit voltage on the secondary of the rectifier transformer.

One can also write an equation similar to (3.5) for the reduced dc system (all buses eliminated except the transfer buses).

$$|I_i| = \sum_{j=1}^{N_T} Y'_{i-1,j}\ C_{j+1}\ |E_{j+1}| \qquad (3.14)$$

$i=2,\ldots N_T+1$

$i \neq N_F$

Combining (3.10) and (3.14) one obtains:

$$E_k \angle\delta_k = 1 - \left[\sum_{\substack{i=2 \\ i\neq N_F}}^{N_T+1} Z_{k,i} \left(\sum_{j=1}^{N_T} Y'_{i-1,j} \, C_{j+1} \, |E_{j+1}| \right) \angle(\delta_i - \phi_i) \right]$$

$$- Z_{k,N_F} \, I_{N_F} \angle(\delta_{N_F} - 90^o) \qquad (3.15)$$

$k=1,2,\ldots N_A$

This non-linear equation has to be solved iteratively to determine the ac bus voltages. The unknown dc bus voltages can be determined using an equation similar to (3.9). Once all the voltages are known, the line flows can be calculated.

3.4 RESULTS OF STUDY ON A SAMPLE SYSTEM

Based on the above analysis, a computer program was written and tried on the same sample system on which the short circuit study was conducted. The one line diagram for the system is given in Fig.2.10. To accelerate the convergence of solution, acceleration factors were used. As indicated in the load-flow analysis an acceleration factor of 1.6 was found to be optimal for that study. However, when acceleration factors in the neighborhood of 1.6 were tried, the solution failed to converge. This behavior was observed for all values of acceleration factors greater than unity. However, when acceleration factors of less than unity were used, the solution converged rapidly. In fact, for the sample system, using an acceleration factor of 0.6, convergence was obtained in only 10 iterations.

The solution obtained for a fault at bus #7 is as follows:

a) Fault at bus 7

b) Number of iterations 10

c) Fault currents through rectifiers

Rectifier #	Current (p.u.)
1	1.340
2	0.266
3	1.420
4	1.204
5	0.143

d) Total fault current = 4.373 p.u.

e) AC bus voltages

Bus #	Voltage (p.u.)
1	0.8475-j0.1548
2	0.8338-j0.1471
3	0.8461.j0.1546
4	0.8200-j0.1391
5	0.8200-j0.1397
6	0.8189-j0.1395
7	0.8246-j0.1419
8	0.8461-j0.1546
9	0.8200-j0.1391
10	0.8189-j0.1395

f) AC line flows

From Bus	To Bus	Current (p.u.)
1	2	2.858-j2.929
1	3	0.239-j0.118
2	7	1.942-j1.953
3	8	0-j0
4	9	0-j0
4	7	-0.951+j1.053
7	5	0.987-j0.900
5	6	0.134-j0.052
6	10	0-j0

g) DC bus voltages

Bus #	Voltage (p.u.)
1	0.6782
2	0.8266
3	0.6532
4	0.6805
5	0.8126
6	0.6532
7	0
8	0.7413
9	0.7413
10	0.8126

h) DC line flows

From Bus	To Bus	Current (p.u.)
1	7	1.474
3	7	1.420
3	6	0
7	4	-1.479
4	5	-1.436
5	10	0

h) DC line flows (continued)

From Bus	To Bus	Current (p.u.)
4	8	-0.132
8	9	0
2	8	0.123
1	2	-0.134

3.5 CONCLUSIONS RELATED TO AC/DC ANALYSIS

The algorithms developed here are specifically meant for the analysis of coal mine power systems. However, they can be used for any industrial power system using ac/dc distribution, such as a transportation system, without any major modification.

The load-flow analysis will help one in choosing the size of the trolley wire, rectifier rating, their spacing along the track and size of cables, etc. Similarly, the short circuit analysis will help in choosing interrupter ratings and help design an effective protective relaying scheme for the power system.

CHAPTER IV

MINE POWER SYSTEM SIMULATOR

To experimentally verify the results obtained by computer analysis, a scaled-down version of a small coal mine power system is being built. Simplified models of the following system components have been developed:

1. High- and low-voltage cables.
2. Variable power and power factor ac loads.
3. DC trolley wire system.

The model simulates a power system of a small coal mine consisting of the following:

1. One main substation.
2. Two ac mine power centers.
3. Two rectifiers.
4. High- and low-voltage cables.
5. DC track haulage system.

The block diagram of the system modeled is shown in Fig. 4.1. To start with the design, an actual system was decided upon with the values and sizes of components as shown in Fig. 4.2.

It was decided to build the model using a supply voltage of 240 volts line-to-line, because of its availability in the power systems laboratory at West Virginia University. The secondary voltage at the substation was chosen as 120V (line-to-line) and at the utilization level as 20V (line-to-line). These voltage levels were primarily chosen due to the availability of components such as transformers, etc.

The three-phase schematic of the model is given in Fig. 4.3(the assembly of the model is almost 90% completed). Once the model is fully assembled, load-flow and short circuit studies will be performed and compared with theoretical analysis.

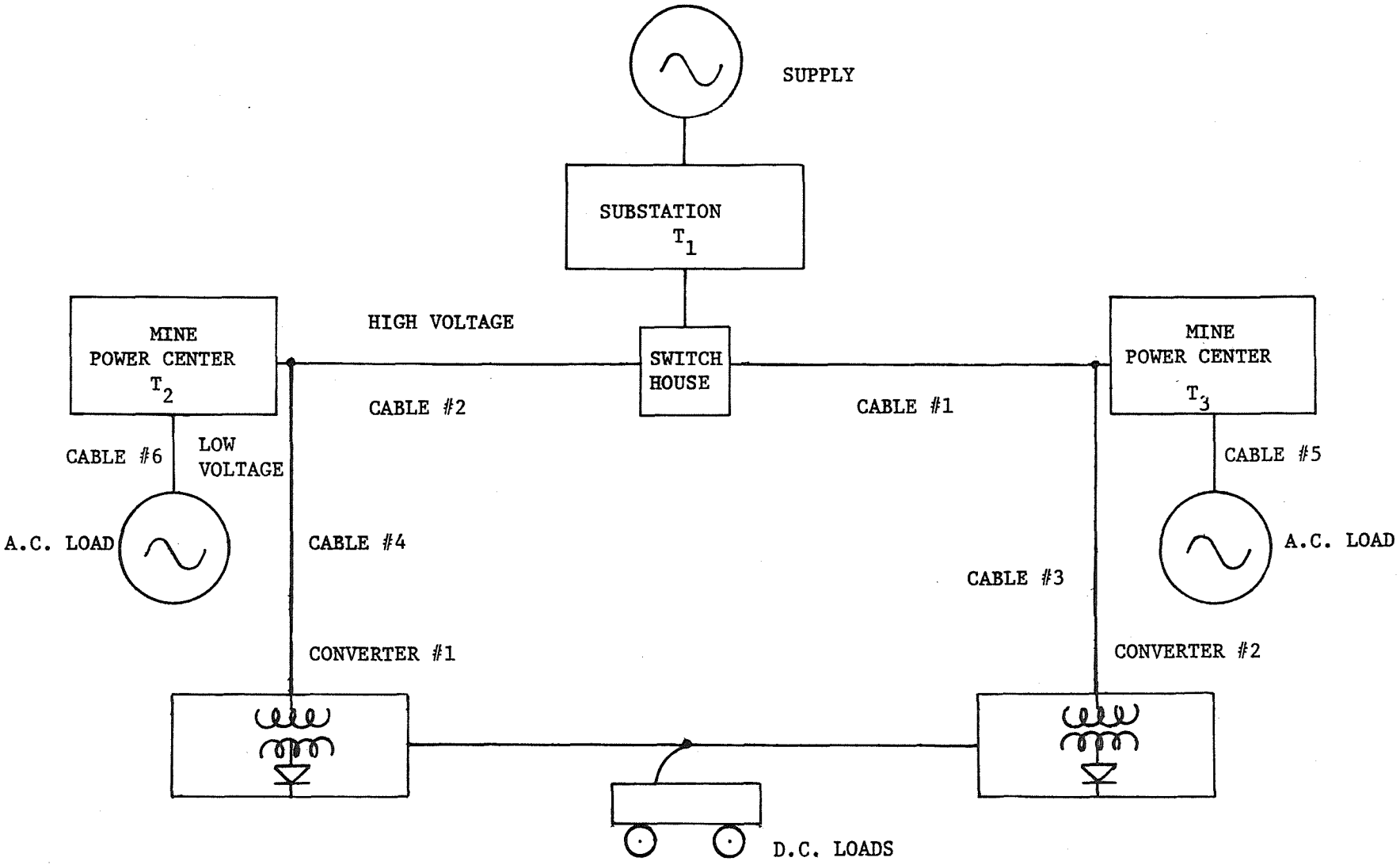

Fig. 4.1 **Block Diagram of the System being Modeled.**

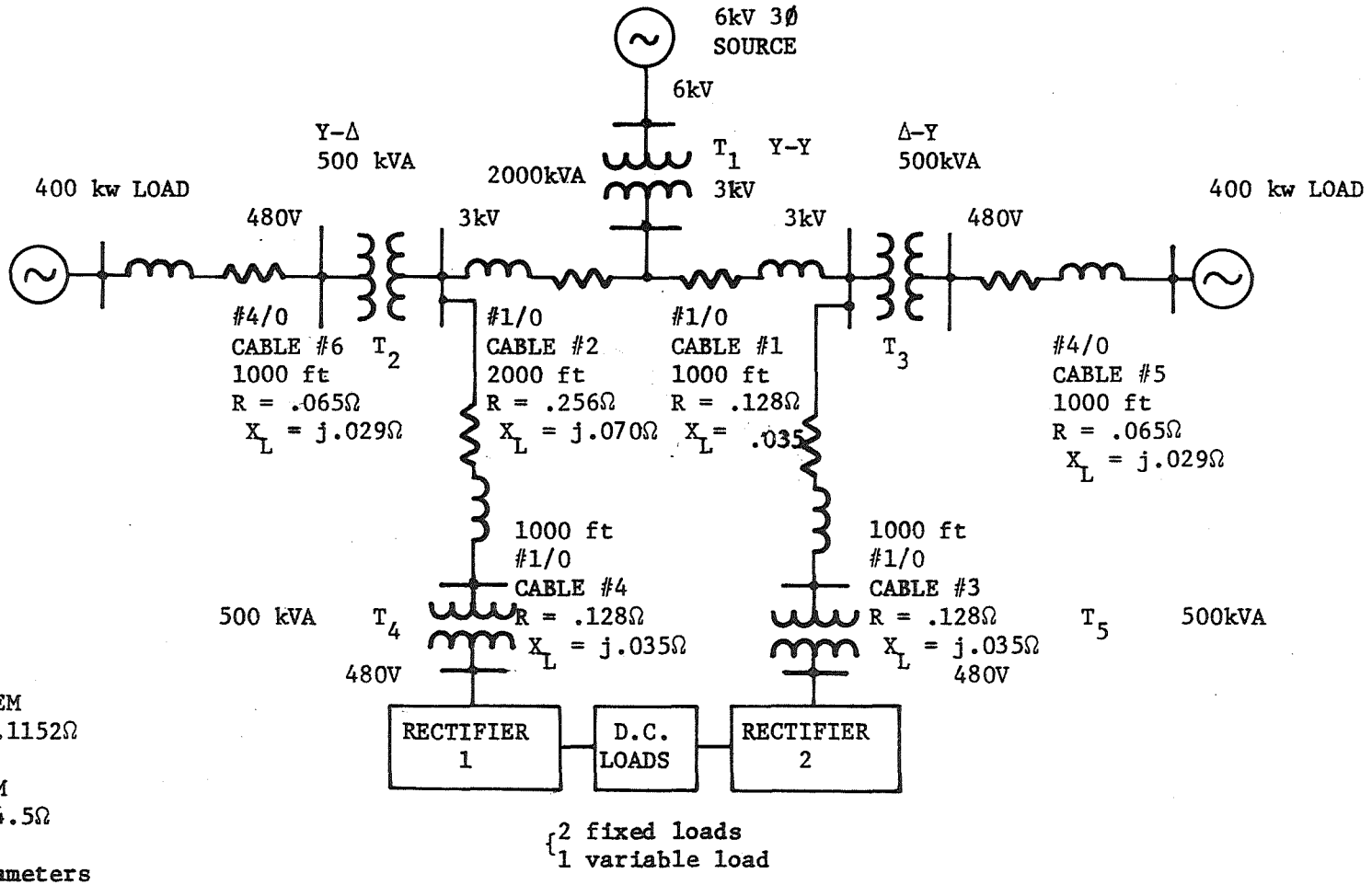

480V SYSTEM
Base Z = .1152Ω

3kV SYSTEM
Base Z = 4.5Ω

Cable parameters
per 1000 ft

SIZE	R	X_L
#1/0	.128	j.035
#4/0	.065	j.029

Values in Ohms

Fig. 4.2 Single Line Diagram of the System Being Modeled.

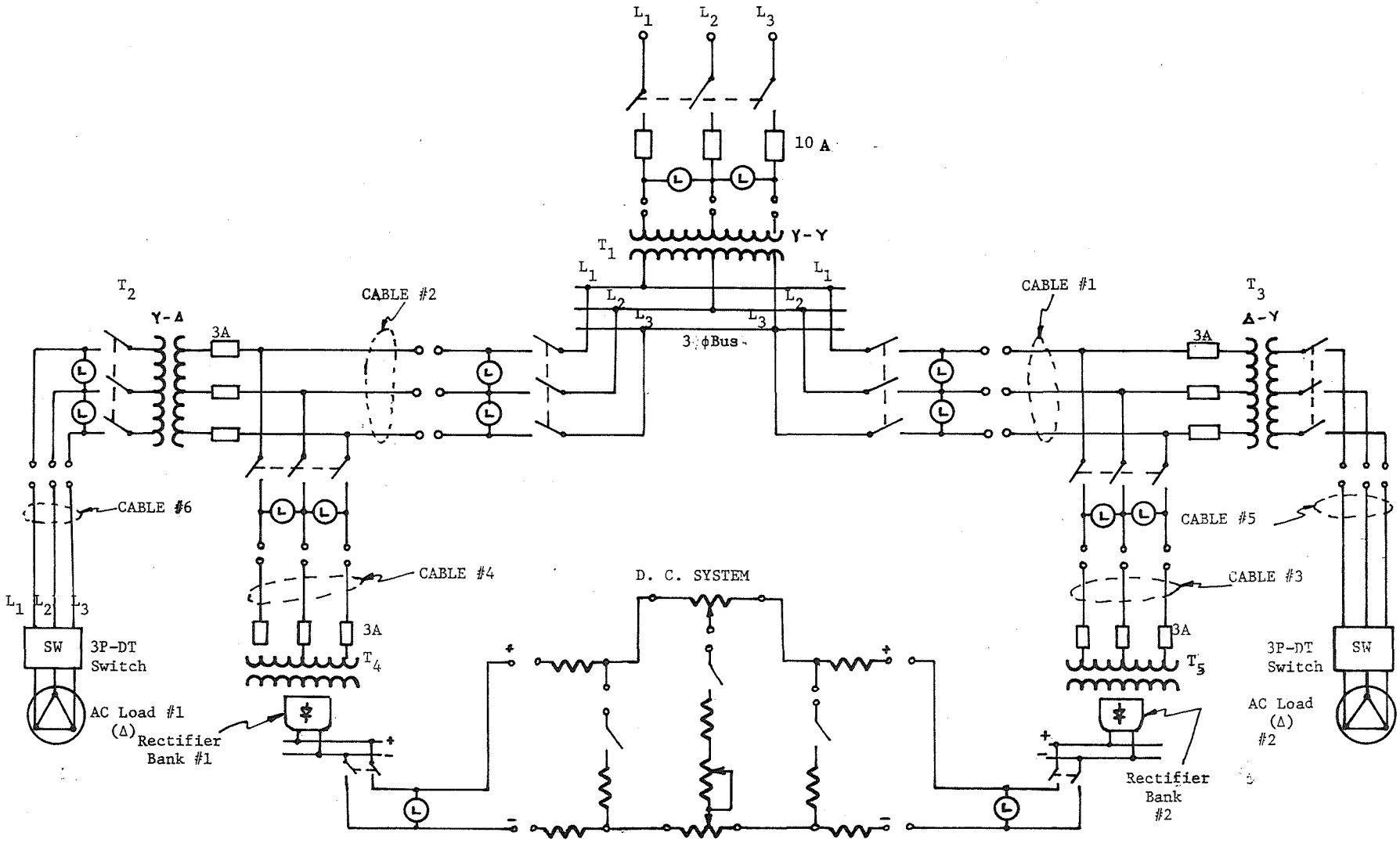

Fig. 4.3. 3 Detailed Schematic of the Model

CHAPTER V

SIZING OF POWER CABLES FOR CYCLIC LOADS

5.1 INTRODUCTION

A typical coal mining equipment constitutes a continuously variable electrical load. The power drawn from the system depends on the mining operation being carried out and is cyclic in nature. The typical duration of a load cycle is 3-4 minutes. It is quite short compared to the time constant of the power cable feeding it, which is of the order of 40 minutes. Since the equipment is in a state of constant motion, the power cables feeding it from the coal mine power center are portable. The typical length of the cable is approximately 500 ft.

The ampacity ratings specified by cable manufacturers are based on continuous current carrying capability. Thus, there is very often a tendency in coal mining applications to oversize the cable. This might be good from the system performance point of view due to reduced cable temperatures, losses and voltage drop, but is nevertheless an unnecessary economic burden. Also, the larger the size of the cable, the more difficult is its movement and handling within the coal mine.

In this analysis a simple thermal-electric model of a round low-voltage power cable is derived. Equations are developed describing the behavior of the cable under cyclic electrical load and solution presented. A method is described to optimally size the cable subject to the various operating constraints such as allowable cable temperature rise, maximum ambient temperature, maximum length of cable and allowable voltage drop.

Effects of change of conductor resistance due to change in temperature are also taken into account. However, in the analysis presented it is assumed that the load-time characteristics of the equipment under consideration are fully known.

5.2 DUTY CYCLES OF VARIOUS COAL-MINING EQUIPMENT

A recent study [5] was conducted by the Pennsylvania State University to determine the various operating characteristics of coal-mining machinery. It was found that for some of the machinery like the continuous miner, the input electrical power was highly variable, depending on the operation it was performing. A typical load-time characteristic of a 400hp continuous miner is given in Fig.5.1. It was also found that on an average, continuous miners operate only 40% of the time. They idle for the rest of the time, during which they draw very little power. Also, it was revealed that the mining equipment generally operates on very low power factors. This is due to the fact that the motors are not always fully loaded. A typical power-factor vs. loading curve for a class B induction motor is given in Fig.5.2. It is seen that the power factor rises from about 0.15 at no load to about 0.80 at full load.

The best fit for this curve using least square[5] estimation was found to be:

$$\cos \phi = 0.85 - 0.70\, e^{-2.2p} \qquad (5.1)$$

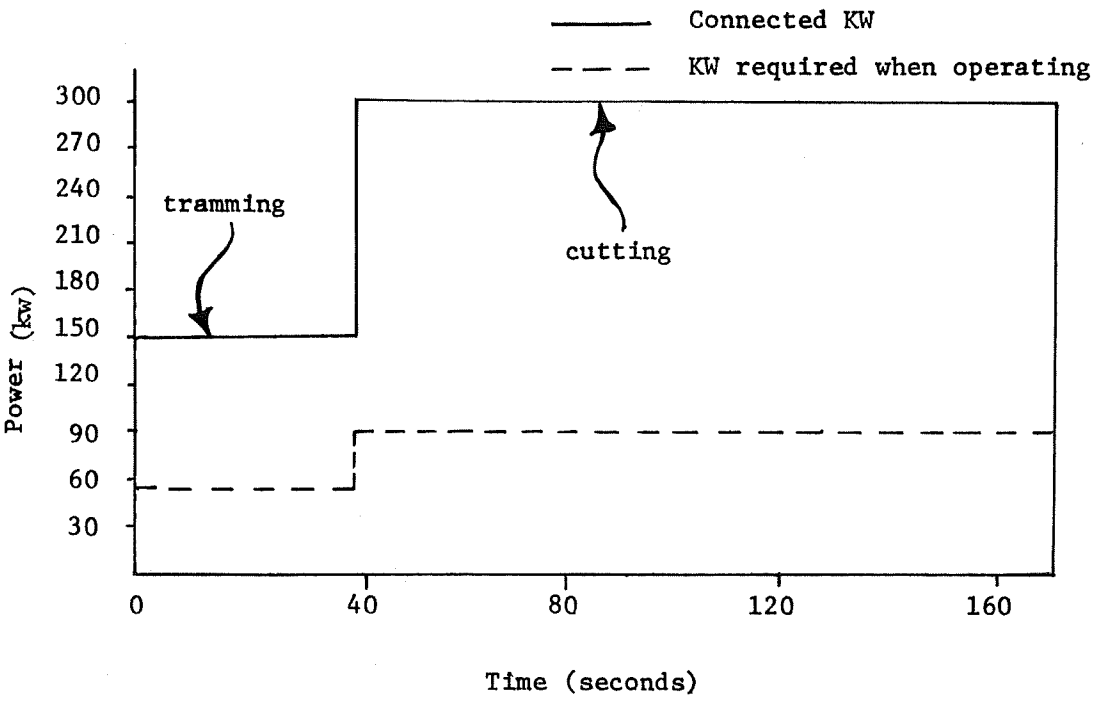

Fig. 5.1 Average Duty Cycle of a 400 HP Continuous Miner (From Reference 5)

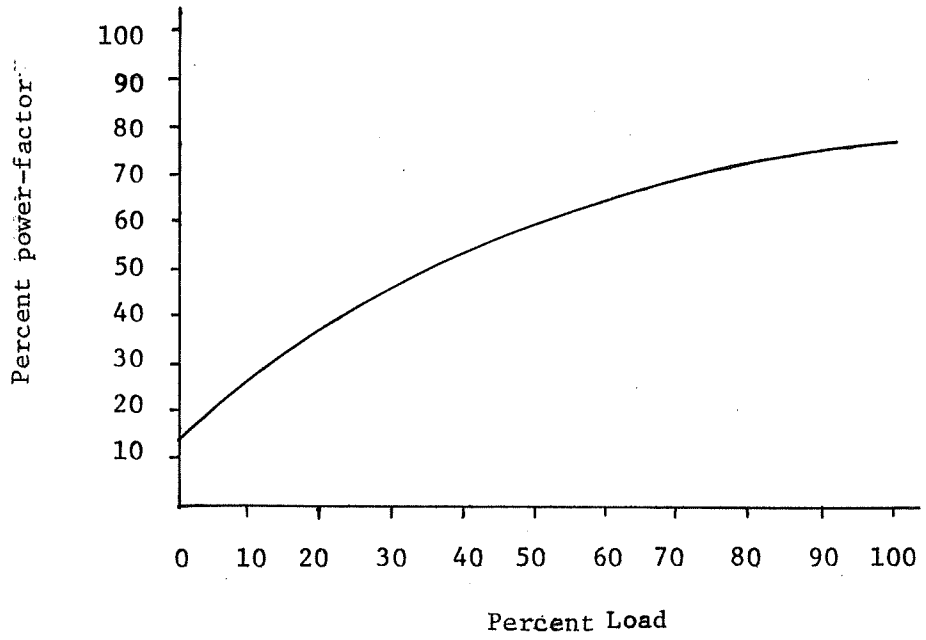

Fig. 5.2 Variation of Power-Factor With Load for Design B Squirrel Cage Induction Motors (From Reference 6)

where:

$\cos \phi$ is the operating power factor of the motor
p is the per-unit loading

Hence, if one knows the loading on a motor, one can determine the approximate power factor using the above equation.

5.3 FACTORS AFFECTING CABLE SELECTION

Once the duty cycle (power and power-factor vs. time) of an equipment is fully known, one has to go about selecting a proper size cable to feed power to it. The following factors have to be taken into account when proceeding with the cable selection.

1. Maximum allowable conductor temperature rise.
2. Allowable voltage drop.
3. I^2R losses within the conductor.

These factors will now be fully analyzed.

5.4 TEMPERATURE RISE IN A CABLE

As current flows through a cable, the temperature both inside the cable and at the surface rises due to the I^2R losses. The temperature reaches a steady state when the heat generation equals the heat loss due to convection and radiation. It is well known that the temperature rise vs. time is an exponential curve. A typical temperature rise curve is given in Fig. 5.3. Mathematically, it can be expressed as

$$T(t) = T_s + (T_A - T_s)\, e^{-t/t_c} \qquad (5.2)$$

where:

$T(t)$ is the temperature after time t.
T_s is the final steady-state temperature and depends on the current flowing through the cable.
T_A is the initial or the ambient temperature.
t_c is the time constant of the cable and is equal to the time taken to reach 63.2% of the final steady-state temperature rise. It is independent of the magnitude of current flowing through the cable.

It is assumed that all the temperatures are measured on the surface of the cable.

Suppose, instead of a steady load, the cable is feeding a cyclic load, such as a continuous miner. Knowing the time duration of each operation within the cycle, one can use equation 5.2 for each operation, except that T_s has to be determined for each operation. Also, $T(t)$ calculated at the end of one operation will become T_A for the beginning of the next operation, and so on.

Of the unknowns in equation 5.2 , t_c can be determined easily by heat run

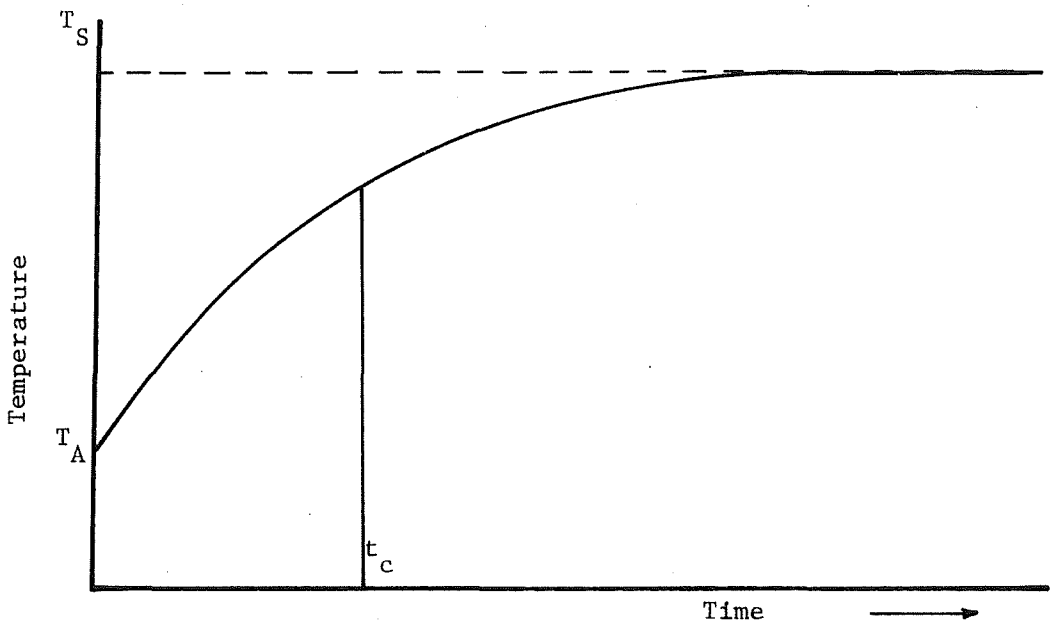

Fig. 5.3 Typical Temperature Rise Curve for a Power Cable.

tests on the cable. However, it is difficult to determine T_s as a function of current, because it would involve conducting several tests for different values of the current. Also, one is interested in finding the maximum conductor temperature, (T_c), since it is one of the limiting factors in sizing a cable. To determine these, a simple steady-state thermal model was developed which will be discussed below.

5.5 DEVELOPMENT OF A STEADY-STATE THERMAL MODEL

The heat generation within a cable is non-uniform due to the geometry of the cable. Hence, the temperature inside the insulation as a function of the radial distance from the center will not be the same in all the directions. Fig.5.4 shows the cross-section of a power cable and the temperature contours. To accurately model this temperature distribution would involve the use of finite element analysis and quite involved programming, which is not the intent of this research.

However, at steady-state, as one approaches the surface of the cable, the temperature tends to equalize and all the points on the surface are almost at the same temperature. This is analagous to an equipotential in an electric field. Viewed from the surface, the source of heat (conductors) looks like a concentric cylinder. Hence if one can find an equivalent radius of this concentric cylinder, one might be able to model the heat transfer within the cable to an acceptable degree of accuracy. However, this model would only be able to predict the maximum conductor and surface temperatures and not the temperature distribution within the cable, which is the intent.

The heat transfer by the conductors to the insulation is a surface phenomenon. Approximately 5/6 of each conductor surface is involved in heat transfer to the insulation. The diameter of the equivalent cylinder should be such, so that the total heat transfer surface is the same in both the cases.

$$3 \times 5/6 \times 2\Pi\, r_c = 2\Pi\, r_1 \qquad (5.3)$$

where

r_c is the radius of each conductor

r_1 is the radius of the equivalent cylinder

It follows from equation 5.3 that

$$r_1 = 2.5\, r_c \qquad (5.4)$$

Thus, knowing r_c one can find r_1.

The concentric cylinder model is shown in Fig.5.5. This model is used in the analysis of the heat transfer problem. The following symbols are used:

D outside diameter of the cable, in cm
I rms value of the current, in A
E emissivity of cable insulation ($\simeq$ 0.95)
K coefficient of thermal conductivity of cable insulation, in W/cm- °C

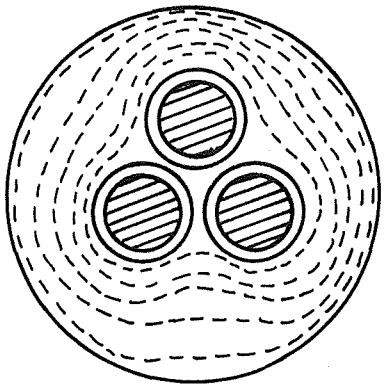

Fig. 5.4 Cross Section of a Cable. The Dotted Lines Represent Temperature Contours.

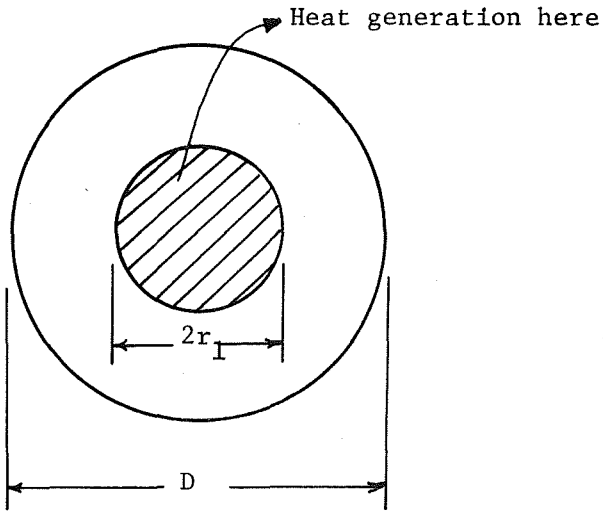

Fig. 5.5 Equivalent Concentric Cylinder Model for the Table.

T_A ambient temperature, in °C

T_S steady-state surface temperature of the cable, in °C

r_1 radius of equivalent cylinder, in cm

$R(T)$ resistance of the conductor per unit length at any temperature T, in Ω/cm

T_R reference temperature at which the resistance value is given, in °C

T_C steady state conductor temperature, in °C

At steady state:

Heat generated within the cable = Heat conducted through the insulation
= Heat dissipated due to radiation and convection

$$\text{Heat generated/unit length} = 3I^2 R(T_C) \text{ W/cm} \tag{5.5}$$

$$\text{where } R(T_C) = R(T_R) \frac{(234.5+T_C)}{(234.5+T_R)} \tag{5.6}$$

$$\text{Heat conducted through the cable/unit length} = \frac{2\Pi K (T_C-T_S)}{\ln (\frac{D}{2r_1})} \text{ W/cm} \tag{5.7}$$

From equations 5.5 , 5.6 and 5.7

$$T_S = T_C - \frac{3}{2\Pi K} \ln (\frac{D}{r_1}) \frac{I^2 R(T_R) (234.5+T_C)}{(234.5+T_R)} \tag{5.8}$$

This equation gives the relationship between the surface and conductor temperatures at steady state.

Heat loss due to radiation/unit length

$$= 5.72X10^{-12} e(T_S+273)^4 - (T_A+273)^4 \Pi D \text{ w/cm} \tag{5.9}$$

Assuming natural convection in free air :

$$\text{Heat loss due to convection/unit length} = 4.172X10^{-4} (T_S-T_A)^{5/4} \Pi D^{3/4} \text{ W/cm} \tag{5.10}$$

From equations 5.5 , 5.6 , 5.9 and 5.10

$$3I^2 R(T_R) \frac{(234.5+T_C)}{(234.5+T_R)} = 5.72X10^{-12} e\Pi D ((T_S+273)^4 - (T_A+273)^4) + 4.172X10^{-4} (T_S-T_A)^{5/4} \Pi D^{3/4} \tag{5.11}$$

The value of the surface temperature can be substituted in terms of the conductor temperature from equation 5.8 . Thus, one gets a nonlinear equation in terms of T_C alone. This can be solved by the Newton's iterative method to determine T_C and then T_S, which are the steady-state values of the conductor and surface temperatures, respectively.

5.6 EXPERIMENTAL VERIFICATION OF THE MODEL

Presently, an effort is being undertaken to verify the results of the thermal model by experimental analysis. Thermocouples are inserted to different depths within the cable insulation to get an idea of the temperature distribution. The thermocouples used are copper-constantan and are made of 36 gauge wire. Holes approximately 1 mm in diameter are drilled in the cable to insert the thermocouples. The diameter of the holes is kept to a minimum to avoid any heat loss through it.

To measure the surface temperature, six thermocouples were placed on the surface at different locations. The surface temperature rise for an AWG2 cable, which was subjected to a current of 200A, is plotted in Fig. 19. Note that this is the average of all the thermocouple measurements. The difference between maximum and minimum temperatures at the surface during steady-state was found to be 5°C. For measuring the conductor temperature, the thermocouples were inserted into the cable until they touched the power conductors. The temperature rise curve for the conductors is given in Fig. 20. Again, this is the average of all the measurements.

Looking at Figs. 5.6 and 5.7 one can note that the steady-state surface temperature is 67°C and the conductor temperature is 102°C. The values predicted by the model are 66°C and 96°C, respectively. Hence, it seems that the measured and predicted values show good correlation. Testing is continuing to gather more data and arrive at a firm conclusion.

5.7 VOLTAGE DROP ANALYSIS

The connection of the machine to the power center is indicated in Fig. 5.8. V_S is the sending end voltage (assumed to be fixed) and $V_R(t)$ is the receiving end voltage. R and X_L are the cable resistance and reactance, respectively. All quantities are in per unit on any given base. It is assumed that fixed power factor correction capacitors are provided at the machine. Right now such a practice is not followed due to the inflammable nature of power capacitors. They are included in the analysis only to show the saving they can effect in terms of cable size, reduced cable temperatures and power loss.

The complex power flow in the cable is given by:

$$P(t)+jQ(t) = [Kw(t)+jKw(t)\ \mathrm{Tan}\ \Theta\ (t)] - j\mathrm{kvar} \qquad (5.12)$$

where

P(t)	is the real power flow in the cable
Q(t)	is the reactive power flow
Kw(t)	is the real power consumed by the machine
$\Theta(t)$	is the power factor angle at the machine
kvar	is the reactive power (leading) due to power factor correction capacitors

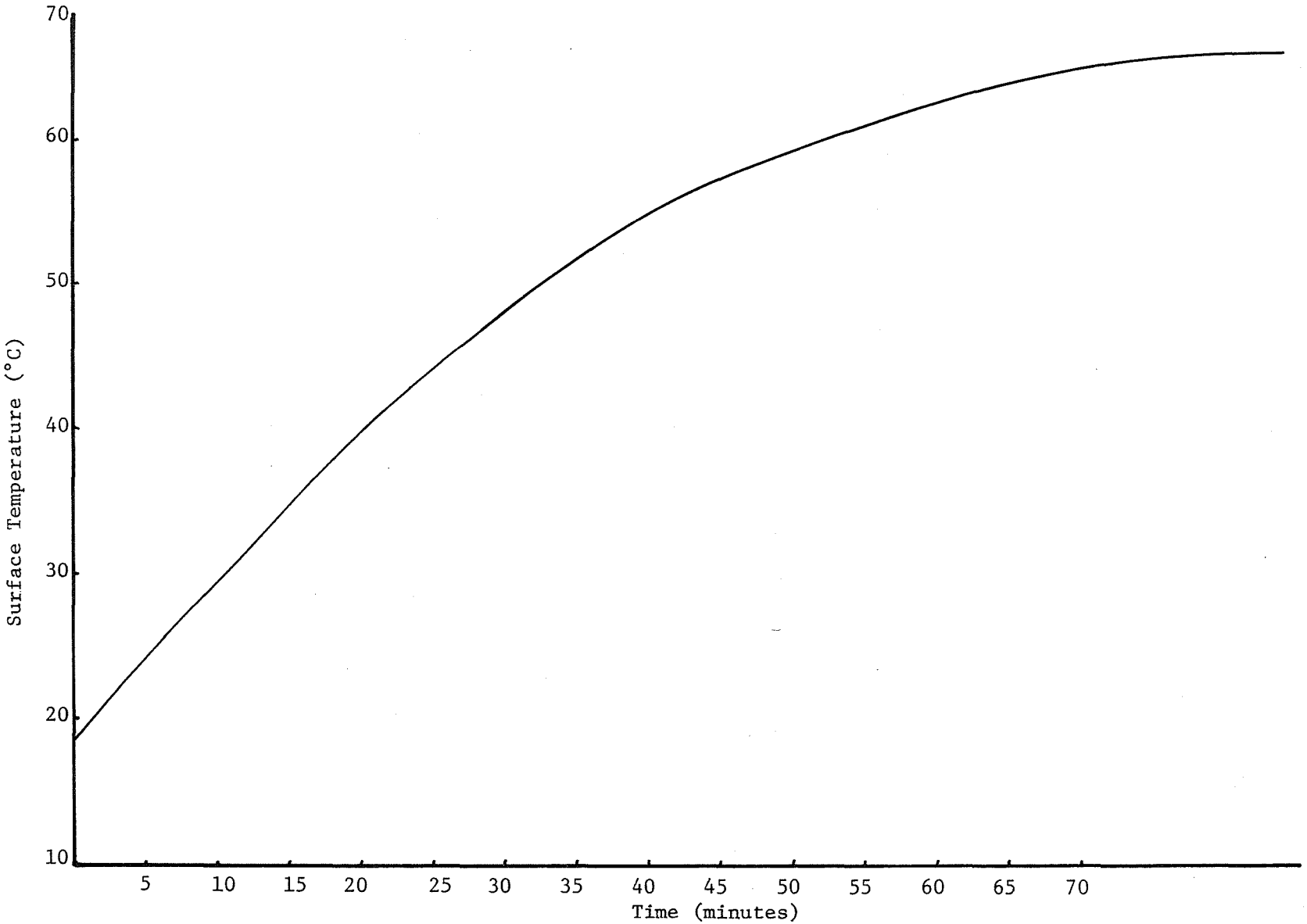

Fig. 5.6 Surface Temperature Rise for a AWG 2 Cable Subjected to a Current of 200A.

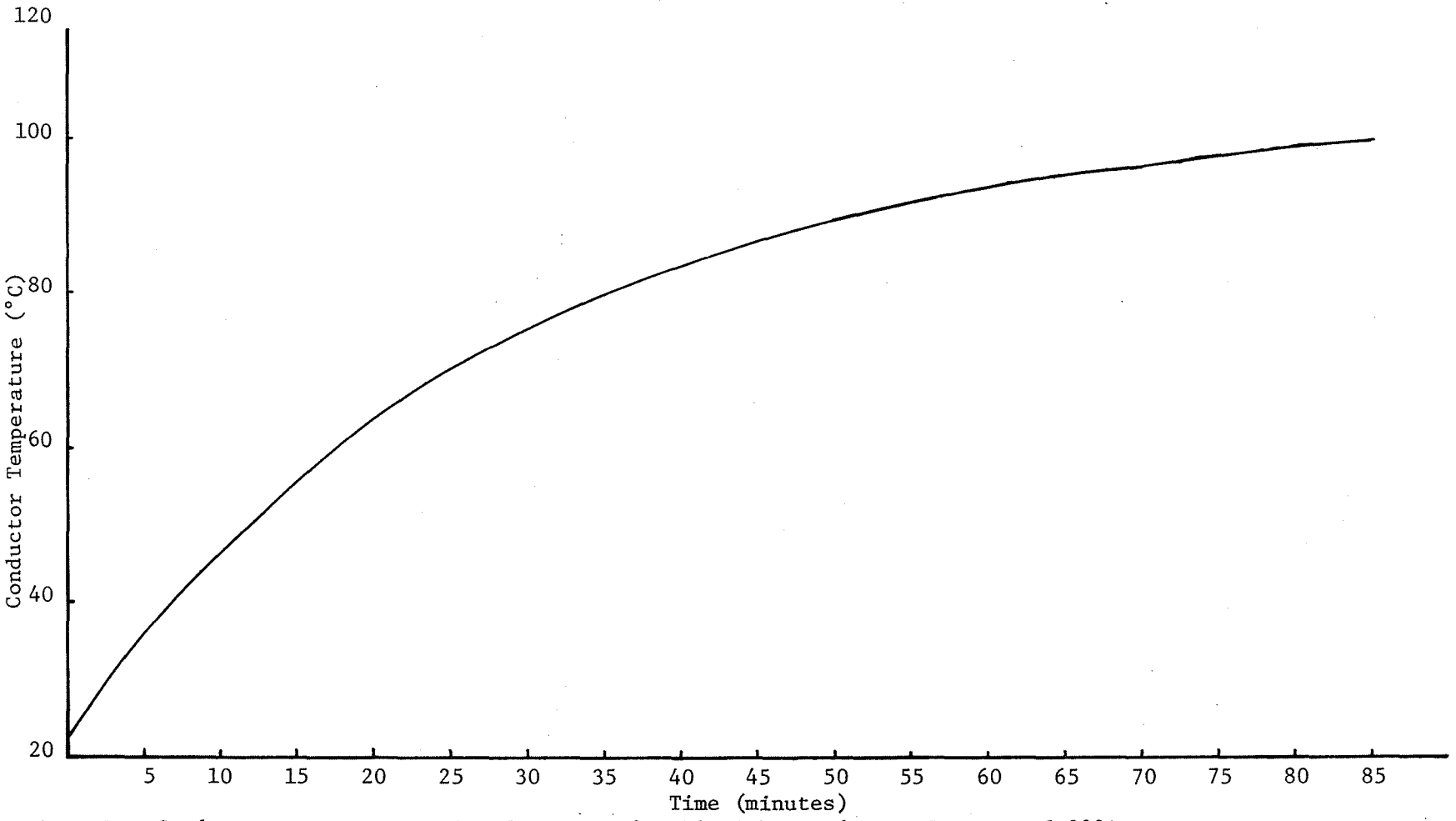

Fig. 5.7 Conductor Temperature Rise for a AWG 2 Cable Subjected to a Current of 200A.

All the quantities are in per-unit and are functions of time because the load is assumed to be cyclic. The capacitors are assumed to be fixed. However, if they are switched with the motors, equation 5.12 may have to be modified slightly.

Let I(t) be the current flowing in the cable. One can find P(t) and Q(t) from equation 5.12 since all other quantities are known. Thus one can write:

$$P(t)+jQ(t) = V_R(t)\ I^*(t)$$

Thus

$$I^*(t) = \frac{P(t)+jQ(t)}{V_R(t)}$$

$$I(t) = \frac{P(t)-jQ(t)}{V_R(t)} \qquad (5.13)$$

The relationship between the sending and the receiving end voltages can be expressed as:

$$V_s = V_R(t)+I(t)(R+jX_L)$$

$$= V_R(t) + \frac{(P(t)-jQ(t))(R+jX_L)}{V_R(t)}$$

$$= \left[\ V_R(t) + \frac{P(t)R}{V_R(t)} + \frac{Q(t)X_L}{V_R(t)}\ \right] + j\left[\ \frac{P(t)X_L}{V_R(t)} - \frac{Q(t)R}{V_R(t)}\ \right] \qquad (5.14)$$

This equation is non-linear and has to be solved iteratively for $V_R(t)$. Once $V_R(t)$ is determined, one can find I(t) and the maximum voltage drop in the cable.

5.8 COMPUTER PROGRAM

The above analysis is incorporated into a computer program to aid in selecting a cable for a cyclic load. The input needed for the program is the duty cycle for the particular piece of equipment, size of power factor correction capacitors, maximum length of the cable and the expected ambient temperature.

The program then calculates the various parameters, such as the maximum conductor temperature, voltage drop, etc., for various cable sizes. Thus, one can select a cable which meets all or most of the design specifications.

5.9 RESULTS FROM A SAMPLE PROBLEM

The program is used to select a cable for an equipment whose duty cycle is given in Fig.5.9. Two analyses are performed; one with no power factor correction capacitors and another with 100 kvar of capacitors at the machine.

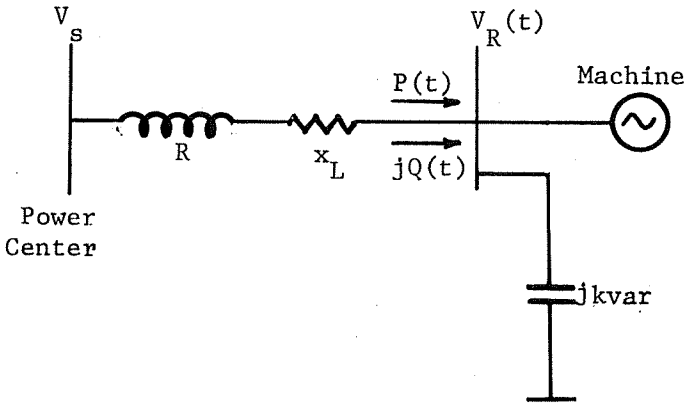

Fig. 5.8. Connections of the Machine to the Power Center.

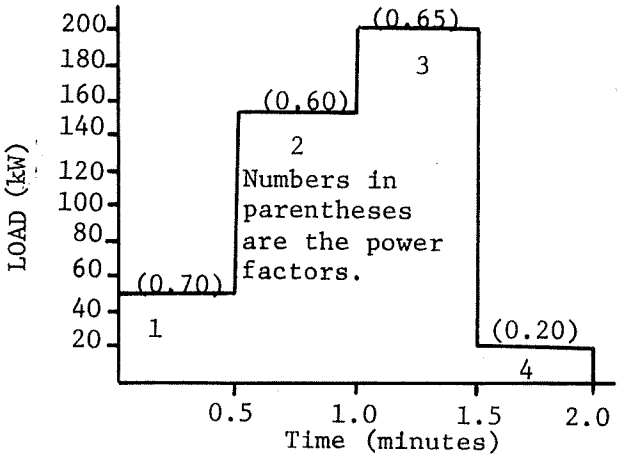

Fig. 5.9 Duty Cycle for the Load of Sample Problem.

The duty cycle has a total duration of 2 minutes and has 4 operating regions. With no capacitors, the currents for the various regions were calculated as 85, 300, 375, and 120 amperes, respectively. If one were to choose a cable for maximum expected value of current (375A), one would probably choose a 350 MCM cable. Similarly, with 100 kvar capacitors present, the currents were calculated as 84, 216, 289, and 24 amperes, respectively.

The program further calculated the different operating parameters for various cable sizes. Results obtained are indicated in Table 5.1 for the case with no capacitors and Table 5.2 with capacitors present.

TABLE 5.1

Cable Size	Maximum Voltage Drop (percent)	Power Loss per Cycle (kWh)	Maximum Surface Temperature (°C)	Maximum Conductor Temperature (°C)
3/0	10.00	0.171	63.43	80.73
4/0	8.29	0.132	57.30	70.82
250MCM	7.37	0.108	52.35	62.82
350MCM	5.9	0.076	47.68	54.24

TABLE 5.2

Cable Size	Maximum Voltage Drop (percent)	Power Loss per Cycle (kWh)	Maximum Surface Temperature (°C)	Maximum Conductor Temperature (°C)
1/0	12.87	0.148	62.81	77.59
2/0	10.35	0.115	57.04	68.31
3/0	8.33	0.089	52.34	60.60
4/0	6.82	0.070	49.03	55.48

Assuming that the operating constraints are a maximum insulation temperature of 75°C and a voltage drop of 10%, one would have to use a 4/0 cable with no capacitors present and a 2/0 cable with 100 kvar of capacitors.

5.10 CONCLUSIONS RELATED TO CABLE AMPACITIES

A steady-state thermal model for a three-phase power cable is presented. The validity of the model is being established by tests in the laboratory.

Based on the model, a method to select a cable for a cyclic electrical load, such as a continuous miner, is given assuming that the load characteristics are fully known.

REFERENCES

1. J. Reeve, G. Fahmy, and B. Scott, "Versatile Load Flow Method for Multi-terminal HVDC Systems", IEEE Trans. Power Apparatus and Systems, Vol. PAS-96, May 1977, pp 925-33.

2. S. N. Talukdar and R. L. Koo, "The Analysis of Electrified Ground Transportation Networks", IEEE Trans. Power Apparatus and Systems, Vol. PAS-96, Jan. 1977, pp 240-247.

3. E. W. Kimbark, Direct Current Transmission, Vol. I, Wiley Interscience, (1971).

4. G. W. Stagg and A. H. El-Abiad, Computer Methods in Power System Analysis, McGraw-Hill, New York (1968).

5. D. Jeng, M. S. Thesis, Pennsylvania State University, June 1974.

6. D. A. Fink and J. M. Caroll, Standard Handbook for Electrical Engineers.

7. C. C. Barnes, Power Cables: Their Design and Installation, Chapman and Hall, (1966).

8. M. Jakob and G. A. Hawlems, Elements of Heat Transfer, John Wiley and Sons.